Recent Advances in Gun Propellant Development: From Molecules to Materials

Eugene Rozumov

Abstract The development of gun propellants from 2010 to 2016 has been a broad endeavor. Researchers worldwide have examined every facet of energetic materials involved with gun propulsion in efforts to improve both safety and performance. They have looked at individual molecules to maximize energy content, as well as revisiting past molecules and improving upon their original properties. A great deal of effort has gone towards understanding and producing energetic nano-materials. Co-crystallization of energetic materials has also emerged as a promising new methodology to prepare energetics. Processing modifications to the propellant material have shown improvements in burn rate modification. Charge consolidation has seen a resurgence and novel gun concepts have both lead to significant improvements in muzzle velocity at the prototype level. Virtually every aspect of a gun propellant has been examined and improved upon.

Keywords Gun propellant · Energetics · Energetic nano-materials · Energetic co-crystals · Ignition

1 Gun Propellant Ballistics in a Nutshell

The role of gun propellants is to push a projectile out of a tube. The propellant occupies the space in a gun chamber immediately behind the projectile that it is supposed to expel as shown in Fig. 1. It is usually a solid energetic material that upon the application of a proper energy stimulus rapidly decomposes into small gaseous molecules. The subsequent rapid volumetric expansion of the gasses propels the projectile down the bore of the gun. Guns can be characterized by whether their target is hit via a line of sight (small caliber guns, medium caliber guns, tank guns) or non-line of sight (grenade launchers, mortars, artillery)

E. Rozumov (✉)
U.S. Army—Armaments Research Development and Engineering Center (ARDEC), Picatinny Arsenal, USA
e-mail: eugene.rozumov.civ@mail.mil

M.K. Shukla et al. (eds.), *Energetic Materials*, Challenges and Advances in Computational Chemistry and Physics 25, DOI 10.1007/978-3-319-59208-4_2

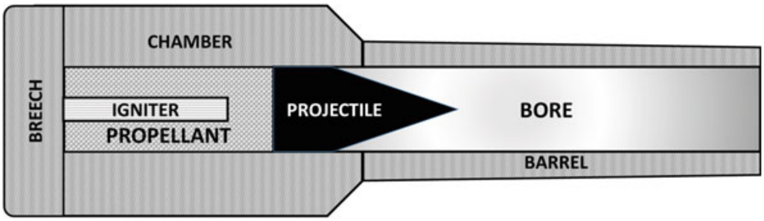

Fig. 1 Basic diagram of a gun

trajectory. Each of these systems has its own set of requirements for maximum chamber pressure, blast over pressure, muzzle velocity, gun barrel erosion, composition of the combustion gasses, and flame temperature. Furthermore, the propellant must be entirely consumed by the time the projectile exits the gun barrel and capable of being safely stored for several decades. Let us also not forget that these gun propellants are also required to ballistically perform the same way in an operating temperature range from −60 to +70 °C.

As an example, mortars have a much thinner chamber wall than any other large caliber gun, and thus have strict requirements for low chamber pressures. The blast overpressure and flame temperature must also be low since the warfighter is standing in close proximity to the muzzle. Gun barrel erosion is not a significant concern owing to the low cost of a mortar gun tube. Once a gun system and the requirements of the propellant are identified, propellant development can begin. As you can see, even though their primary function is quite simple, the requirements that gun propellants must fulfill are quite vast and often competing.

Historically, gun propellants are categorized into three groups. Single base propellants are composed primarily of nitrocellulose, an energetic polymeric binder. The addition of nitroglycerine, a highly energetic and sensitive plasticizer, to nitrocellulose, created a very energetic and hot propellant dubbed a double base propellant. To reduce the flame temperature of a double base propellant, which was necessary to utilize them in large caliber gun applications to extend barrel life, nitroguanidine was added to double base propellant formulations. These propellants consisting of nitrocellulose, nitroglycerine, and nitroguanidine were termed triple base propellants. They are intermediate in energy and flame temperature between single and double base propellants.

A propellant functions by first being ignited at the base of the cartridge or breech of the chamber by an igniter as shown in Fig. 1. Traditional chemical igniters include black powder, boron potassium nitrate ($BKNO_3$), Benite, or clean burning igniter (CBI), which is about 98% nitrocellulose (NC). These materials ignite the propellant bed via a combination of convective heat transfer from the fast moving hot gasses they generate and from conductive heat transfer of hot particles embedding themselves into the propellant grains. The exothermic energy they release is due to the myriad of oxidative combustion reactions that occur during deflagration. Recently, nano-Boron particles were incorporated into a $BKNO_3$

igniter. It was demonstrated that heat output and pressurization rates increased due to the smaller particle sizes, but the maximum pressure generated was not altered by the use of nanoparticles [1].

Once ignited, the propellant undergoes its own combustion reactions laterally from the surface of the grains, filling the gun chamber with more gaseous molecules that push against the projectile base until it exits the gun barrel. Behind the projectile, hot fuel rich gasses are also expelled forming a concentrated plume that is re-ignited upon exposure to atmospheric oxygen owing to its high temperature to produce muzzle flash, which must also be mitigated so as not to give away the position of the gun system [2]. Everything that has been described up until now has to occur in a gun within a few tens of milliseconds.

The pressure versus time trace inside the gun is provided in Fig. 2. The pressure rises and the projectile is pushed into the gun barrel. The projectile begins to move just prior to the chamber pressure reaching a maximum. The pressure inside the chamber rapidly dissipates and while the projectile is moving down the bore and out of the muzzle it is decelerating. To boost gun performance in terms of range, or projectile time of flight, one needs to boost the projectiles muzzle velocity which is directly related to pressure inside the chamber during the ballistic cycle. However, since most fielded guns are already operating at near their maximum pressures, it is not feasible to simply boost the energy of the propellant without modifying the chamber. The optimal way to achieve this would be to widen the pressure time trace without increasing the maximum pressure. This would increase the amount of work performed on the projectile by the propellant gasses thus leading to higher muzzle velocities. To date, a variety of methods involving charge design have been attempted to widen the pressure time curve, but the substantial increase in muzzle velocity has remained elusive.

An alternative approach is to utilize two propellants with significantly different burn rates which would attain maximum pressure at different times, thus in effect increasing the overall pressure experienced by the projectile without surpassing the maximum allowable pressure. One recent approach has been to use a two stage gun design. In this case, the gun chamber contains two propellants, and two igniters,

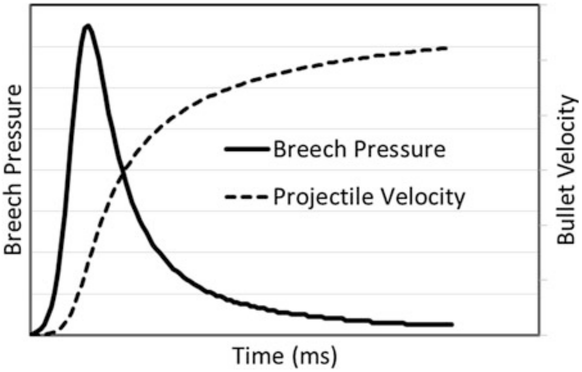

Fig. 2 Pressure and projectile velocity profile during the ballistic cycle

separated by a piston. The propellant adjacent to the projectile is ignited first, which pushes the projectile. Then, a short delay igniter initiated the second propelling charge. The second propelling charge pushes on the piston which then begins to move towards the projectile already moving down the barrel. This compresses the gasses behind the projectile and increases the pressure behind the projectile. This produced a double hump in the pressure time trace, which increased the muzzle velocity by about 30% [3]. Although the increased muzzle velocity was achieved, this gun setup required that the two igniters were part of the breech and barrel. This type of setup requires the development of an entirely new gun system to be practical.

2 Ignition of Propellants

For a gun propellant to function properly and efficiently, its deflagration needs to be initiated. Ideally, the entire propellant bed should be ignited instantaneously, however in practice this is rarely achievable. Besides the chemical ignition methodology described previously, other forms of ignition being examined for gun systems include electrothermal-chemical (ETC) [4], and laser ignition [5]. Both laser and ETC ignition are much more consistent in their delay times than conventional chemical ignition, and offer improved ballistics, but their implementation has been hampered by a variety of reasons.

In ETC ignition, the igniter produces a plasma that imparts its energy directly onto the propellant bed. The benefit of this type of plasma ignition is that ignition delays become very consistent, higher charge loading densities can be efficiently ignited, the entire propellant bed is ignited virtually instantaneously, and the energy input can be compensated to better control ignition during temperature extremes. It has been demonstrated that in a propellant employing plasma igniters, the ignition delay is shortened by about 90%. Furthermore, the plasma achieves similar results to a standard igniter, with less overall energy required. Using a deterred NC strand as an igniter, it was calculated that the NC igniter imparts 2.6 kJ of energy to the propellant based on the calculated heat of explosion under constant volume conditions. The plasma deposited energy was calculated to be 1.05 kJ from the experimental currents and voltages [6].

A variant of ETC known as electrothermal ignition (ETI), incorporates an empty space between the propellant and the formed plasma. This space permits the plasma to become a working fluid before it interacts with the propellant. In a recent study, ETI was employed as an ignition source for a CAB based low vulnerability (LOVA) propellant in a 45 mm laboratory gun at two loading densities (0.5 and 0.7 g/cc) and two temperatures (21 and −40 °C). Gun propellants are known to lose some muzzle energy at extreme cold temperatures leading to reductions in muzzle velocity and subsequent range. It was demonstrated in this effort that ignition delays were indeed reduced, and very consistent. At the lower charge density, the velocity of the projectile at cold temperature was effectively compensated for by the addition of more plasma energy. However, when this technique was employed with the larger loading density, large negative differential pressures (NDP) were observed between the breech of the gun and the projectile base. These were mitigated by lowering the plasma energy at the expense of increasing ignition delays from about 1.5 ms to 3 ms [7].

The occurrence of NDPs is in many cases due to ignition. Because chemical ignition occurs at the base of the chamber and spreads towards the projectile, the bulk propellant is not ignited simultaneously. This in turn leads to pressure waves forming inside the gun chamber. Once the pressure wave travels from the ignition source towards the projectile, it can get reflected back by the base of the projectile. This reflected wave begins raising the pressure significantly behind the projectile and is traveling towards the breech of the gun, thus forming an NDP [8]. This spike in pressure will also force the remaining unburnt propellant to burn even faster, as discussed later, and further exacerbates the situation in the gun chamber. If the NDP is great enough, catastrophic gun failure results. This can be traditionally mitigated by careful propellant formulation, grain, and charge design.

Nakamura and co-workers examined the effects of igniter tube length, igniter tube perforation area, and igniter mass for their ability to generate NDPs from a triple base propellant in a closed vessel fitted with a burst disk and several pressure transducers. They demonstrated that with a Benite igniter (a mixture of black powder and nitrocellulose), longer igniter tubes were able to significantly reduce the NDP magnitude because a larger fraction of the propellant bed was ignited early in the ballistic cycle [9]. Thusly, long center core igniters can help mitigate NDP formation in larger caliber guns.

Thermite compositions consisting of a metal fuel and oxidizer have also been demonstrated to be effective igniters for propellants. Howard demonstrated that a variety of thermite oxidizer and fuel combinations can effectively ignite a disc composed of JA2, a high energy propellant. Furthermore, different combinations of oxidizer and fuel were able to ignite the JA2 in different ways. Some lead to a rapid rise in pressure within the chamber from the JA2 disc while others produced a softer more delayed pressurization [10]. This clearly demonstrated how ignition can control propellant ballistic performance.

Baschung and coworkers compared the nanothermite composition WO_3/Al as an igniter against black powder and plasma ignition in a 60 mm gun with a LOVA propellant. As the prefix implies, nanothermites are composed of nanometer scaled particles of oxidizer (WO_3) and fuel (Al). In conventional thermites, upon activation, the oxidizer and fuel undergo redox reactions that generate tremendous heat. In nanothermites, the increased surface area drastically increases the rate of reaction, thereby releasing tremendous amounts of heat very rapidly. Since no gasses are generated in a thermite reaction, convective heating of the propellant bed is not possible. Convective heating, however, is necessary for efficient ignition of the propellant bed. To alleviate this, the $WO_3/2Al$ nanothermite also had azodicarbonamide added at 10% by weight as a gas generator. They demonstrated that the ignition delays of the nanothermite significantly increased relative to the black powder while the velocity of the projectile and maximum pressure in the chamber remained unchanged. They also demonstrated that the plasma ignition was significantly more consistent with regards to ignition delay, and by once again adjusting the plasma energy, they were able to compensate for poor low temperature performance of the LOVA propellant [11].

Recently two nanothermites were examined for their ability to ignite JA2. Both nanothermite igniters were sandwiched between a JA2 disk and a nanoporous silicon wafer filled with potassium perchlorate. The potassium perchlorate would ignite the thermite, which in turn would ignite the JA2 propellant disc. It was demonstrated that a Bi_2O_3 nanothermite was incapable of igniting the JA2 because it generated high velocity gasses which prevented the hot particles from having sufficient contact with the propellant for heat/energy transfer to occur. A copper oxide thermite on the other hand was successful in igniting the JA2 disk [12].

Su and co-workers utilized a supercritical CO_2 fluid technology to generate a foamed NC igniter with titanium particles (5–15%) embedded in it. The titanium particles would increase the effects of conductive heating, thus igniting the propellant bed in a more efficient manner. In comparison to Benite, they clearly demonstrated that their NC-Ti foamed propellant had a higher burning rate, calculated energy, and a significantly higher maximum pressure. Interestingly, the sample with 10% titanium particles had the highest values for burn rate and pressure, demonstrating that there is an optimal amount of titanium that is beneficial for ballistic performance, while below or above that point the material quickly worsens in performance [13].

3 Combustion of Propellants

In combustion, a material is oxidized to the maximal extent of available oxygen. Combustion is a series of complex redox reactions in which a large molecule is broken apart, atom by atom, to form low molecular weight gasses such as water, nitrogen, carbon monoxide, and carbon dioxide, among others. As an example, the combustion of nitroglycerin (NG) is presented in Eq. 1.

$$2C_3H_5N_3O_9 \rightarrow 6CO_2 + 5H_2O + 3N_2 + 1/2\,O_2 \tag{1}$$

As can be seen, NG is oxygen rich. In this idealized case of combustion, all carbons are converted to CO_2, hydrogens are converted to water, and nitrogens were converted to N_2. However, most gun propellant ingredients have an insufficient amount of oxygen, and the reaction described above cannot go to completion. Therefore, the combustion reactions of gun propellants become more complex.

A quantitative measure of a molecule or material's ability to undergo combustion to form CO_2 is its oxygen balance (OB_{CO_2}). The OB_{CO_2} of an energetic material, provides essential information regarding whether enough oxidizer is present in a molecule or material for it to effectively deflagrate. The formula for oxygen balance follows:

$$\%OB_{\mathrm{CO_2}} = -\frac{1600}{Mol.Wt.}\left(2x + \frac{y}{2} + M - z\right) \tag{2}$$

wherein x is the number of carbon atoms, y is the number of hydrogen atoms, M is the number of metal atoms, and z is the number of oxygen atoms. This value reflects the ability of the material to undergo sustained oxidative combustion to form carbon dioxide. An oxygen balance of zero implies that the material has equal parts oxidizer and fuel. A positive oxygen balance implies that the material is rich in oxidizer and should burn to completion. If a material has a negative oxygen balance, it is fuel rich and will probably not burn to completion. One thing to note is the absence of nitrogen in the equation, since nitrogen preferentially forms N_2, thus not requiring the oxygen for it to undergo oxidative combustion. The more oxygen balanced the molecule/material, the more likely deflagration can be sustained.

Since most energetic materials are slightly oxygen deficient, the prediction of gaseous combustion products based on the idealized case of NG in Eq. 1 are insufficient. The Kistiakowsky-Wilson (K-W) rules treat the formation of CO_2 in a step-wise manner and are applicable towards propellants and materials with an OB greater than −40%. In these cases, carbon is first oxidized to carbon monoxide. Then the remaining oxygen is utilized to convert hydrogen to water. Finally any available oxygen converts the carbon monoxide to carbon dioxide. Once again (and in all subsequent methodologies), all nitrogens are converted to N_2. For propellants with an oxygen balance lower than −40%, modified K-W rules should apply. In this case the primary step is the conversion of hydrogen to water, followed by the step-wise conversion of carbon to carbon monoxide, and carbon dioxide respectively. In all of the described methodologies, any unoxidized carbon and hydrogen is converted to carbon residue, and hydrogen gas. Another methodology that attempts to account for inconsistencies observed during actual gun firings are the Springall-Roberts (S-R) rules. Just like the K-W rules, carbon is first converted to carbon monoxide. Hydrogen is converted to water, and then the carbon monoxide is converted to carbon dioxide. Two other caveats are also present. Firstly, one third of the carbon monoxide formed, is converted to carbon residue and carbon dioxide. Then, one sixth of the original carbon monoxide is converted to more carbon residue and water (assuming that not all of the hydrogens were converted to water) [14]. All of the above described methodologies are shown below for an idealized molecule $C_4H_7O_6N_5$ with an OB of −40% and as can be seen, each one produces different amounts of combustion products for the same molecule. Since gun propellants are essentially gas generators, an accurate prediction of the amounts of gasses formed during deflagration is essential.

$$6C_4H_7O_6N_{5(s)} \rightarrow 18CO_{2(g)} + 6C_{(s)} + 21H_{2(g)} + 15N_{2(g)} \quad (\text{ideal combustion case})$$

$$6C_4H_7O_6N_{5(s)} \rightarrow 24CO_{(g)} + 12H_2O_{(g)} + 9H_{2(g)} + 15N_{2(g)} \quad (\text{K}-\text{W combustion case})$$

$$6C_4H_7O_6N_{5(s)} \rightarrow 21H_2O_{(g)} + 15CO_{(g)} + 9C_{(s)} + 15N_{2(g)} \quad (\text{modified K}-\text{W combustion case})$$

$$6C_4H_7O_6N_{5(s)} \rightarrow 12CO_{(g)} + 16H_2O_{(g)} + 5H_{2(g)} + 8C_{(s)} + 4CO_{2(g)} + 15N_{2(g)} \quad (\text{S}-\text{R combustion case})$$

As discussed above, combustion of propellants may not proceed completely to the formation of carbon dioxide due to insufficient oxygen being present in the molecule or material. An oxygen balance can also be calculated based on the formation of carbon monoxide instead of carbon dioxide as in Eq. 3 and may be more indicative of combustion efficiency. Unfortunately, none of these rules are absolute in predicting the actual combustion products, since in actual gun firings, trace gasses have been reported consisting of various nitrogen oxides and hydrogen cyanide. Thusly, not all of the materials nitrogen's are exclusively converted to nitrogen gas.

$$\%OB_{\mathrm{CO}} = -\frac{1600}{Mol.Wt.}\left(x + \frac{y}{2} + M - z\right) \tag{3}$$

Some common energetic propellant ingredients that will be discussed shortly are presented in Table 1 with their respective oxygen balances, densities and heats of formation. As can be seen, as the nitration level of NC increases, its oxygen balance rises, as does its heat of formation (ΔH_f). In energetic formulations, large positive heats of formation are desirable owing to their high potential energy contributions. Nitroglycerin (NG) is a molecule that has an excess of oxygen. The cyclic nitramines RDX and HMX both have OB_{CO}'s of zero and positive ΔH_f's demonstrating their utility in energetic formulations. It has been shown that OB correlates to the brisance of an energetic molecule, but a similar trend has not been observed in multi-component materials, such as propellant formulations. One other noteworthy trend in the table is that for all molecules except for NQ, the OB_{CO} is positive indicating that there is sufficient oxygen present for those materials to undergo combustion and form CO and water. This would indicate that perhaps OB_{CO} is a more realistic indicator of an energetic materials performance than OB_{CO_2}. It also becomes apparent that neither OB_{CO_2} nor OB_{CO} correlate well with ΔH_f.

Recently, a group demonstrated through modeling and experiment, that below a certain threshold value for oxygen balance of a gun propellant, residue appears

Table 1 Properties of some common propellant energetic ingredients

Energetic	Mol. wt. (g/mol)	Formula	OB_{CO_2} (%)	OB_{CO} (%)	Density (g/cc)	ΔH_f (kJ/mol)
NG	227.09	$C_3H_5N_3O_9$	3.52	24.66	1.59	−371
PETN	316.14	$C_5H_8N_4O_{12}$	−10.12	15.18	1.78	−539
RDX	222.12	$C_3H_6N_6O_6$	−21.61	0.00	1.82	70
HMX	296.16	$C_4H_8N_8O_8$	−21.61	0.00	1.91	75
NQ	104.07	$C_1H_4N_4O_2$	−30.75	−15.37	1.76	−92
NC (12.6% N)	272.38	$C_6H_{7.55}N_{2.45}O_{9.9}$	−34.51	0.73	1.66	−708
NC (13.15% N)	279.66	$C_6H_{7.37}N_{2.64}O_{10.2}$	−31.38	2.95	1.66	−688
NC (13.45% N)	284.15	$C_6H_{7.26}N_{2.74}O_{10.4}$	−29.45	4.34	1.66	−678
NC (14.14% N)	297.13	$C_6H_7N_3O_{11}$	−24.23	8.07	1.66	−653

owing to the incomplete combustion of the propellant. They altered the oxygen balance between −29 and −103% by altering the amount of dibutyl phthalate (an inert material with few oxygens) present. They also demonstrated a strong correlation between nitroglycerin content of the propellant and the pressure inside the vessel during combustion. Higher NG content, oxygen balance, and pressures lead to less residue formation [15].

Once properly ignited, gun propellants burn laterally from their surface. The top of the grain exposed to the hot gasses and particles of the igniter begins to form a condensed reaction phase zone within which oxidative chemical decompositions begin forming lower molecular weight gasses which are expelled laterally away from the propellant. This gaseous efflux gives the condensed phase layer a foamy appearance. This reactive zone also increases the temperature of the propellant grain below it, thus lowering the required activation energy for the material beneath it to undergo a combustion reaction. Immediately above this condensed reaction phase zone, there exists the flame front. Between the flame front and the reaction zone is a dark zone, whose height is determined by the velocity of the gasses coming off of the propellant grain and the pressure experienced within the combustion vessel [16].

Since propellant grains burn laterally from exposed surfaces, their burn rate would need to be determined to effectively harness their energy release. A closed vessel (CV) test is usually performed to achieve this. Just as the name implies, it is a completely closed vessel built to withstand enormous pressures. Strand burner tests can also be utilized but are more suited for the lower chamber pressures associated with rocket propellants. From this CV test, in which a fixed amount of propellant grains of known geometry are ignited, and allowed to deflagrate, the burn rate of the propellant can be determined at varying pressures. Furthermore, the coefficients of Vielle's law (Eq. 4) for burn rate can be determined.

$$r = \beta P^{\alpha} \tag{4}$$

For gun propellants, a pressure exponent (α) > 1 implies that the propellant's burn rate is very sensitive towards pressure. Thus, as a propellant with (α) > 1 deflagrates inside the test chamber, the burn rate increases faster than the pressurization. This may be indicative that the material can undergo a deflagration to detonation transition in some cases. Energetic materials that have an (α) < 1 are fairly irresponsive towards pressure changes and are desirable. Black powder falls into this latter category, which is what makes it a very useful igniter. It allows the black powder to be utilized effectively in igniters in virtually any configuration such as bag charges since they do not need pressurization to effectively form flames and hot particles.

It has been demonstrated that CV analysis is quite sensitive towards the testing conditions. An increase in the amount of igniter material employed, changes in the propellant loading density, how the igniter and propellant are packaged, and the dimensions of the CV all play a critical role in determining the burn rate parameters of the propellant. Furthermore, when the burn rate data from the various firing configurations was used to compute the ballistic profile of a 7.62 mm round, none of the closed vessel predicted burn rates permitted an accurate match to the experimental gun firings, thereby indicating that the CV test does not mimic the intended system sufficiently well, and requires further fitting factors to be employed [17]. It is imperative that when comparing burn rates from the literature, the entire procedure for propellant sample preparation is provided.

Variants of the closed vessel test exist, and also provide meaningful information. Interrupted burning of propellants can be achieved by placing burst discs in the CV apparatus which burst and depressurize the chamber after it reaches a critical pressure. The rapid depressurization quenches the deflagration leaving partially burnt propellant. Thus, partially burned grains can be examined. In this manner, multi-perforated propellant grains were demonstrated to exhibit wave-like deflagration inside the perforations instead of uniform lateral deflagration [18].

Based on all of the above information, grains can be designed in which the pressurization rate can be tailored to meet the specific gun requirements. Since deflagration occurs at the surface of a grain, it is directly related to the available surface area. As a spherical or cylindrical grain burns, the available surface area diminishes as shown in Fig. 3. Since there is less available surface area as the deflagration proceeds, the burn rate and pressurization slows down. This is termed regressive burning. Neutral burning can be achieved by adding a single perforation down the middle of a cylindrical grain. Thus, as deflagration proceeds, the outside layer of the grain diminishes in surface area, while the perforation grows in diameter, thus compensating for the lost surface area from the outside of the grain. Multiple Perforations can also be employed to make a propellant exhibit progressive burning, in which the surface area increases as deflagration proceeds. By utilizing multi-perforated cylindrical grains, the increased surface area inside the multiple perforations over compensates for the reduced surface area of the outer grain leading to rapid pressurization until the grain falls apart into slivers, at which point it undergoes regressive burning.

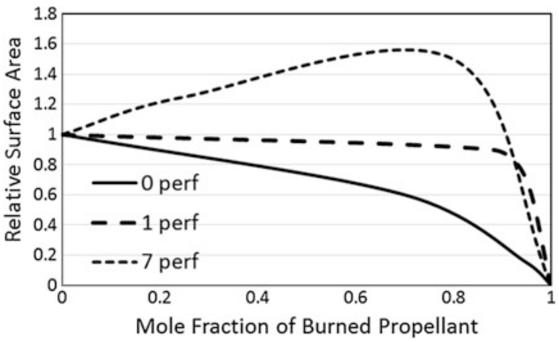

Fig. 3 Effects of grain geometry on available surface area during propellant combustion

4 Propellant Ingredients

4.1 *Energetic Molecules*

What makes a material, and a molecule energetic? By definition, an energetic material is one that contains a large amount of stored chemical energy. When exposed to a sufficient shock, thermal, or impact stimulus, which can overcome the initial activation energy of these materials, they rapidly release this stored energy in an exothermic process. This exothermicity provides the energy for subsequent energetic molecules to overcome their activation energy barriers and the cascade of energy release continues. Therefore, a useful thermodynamic parameter to gauge the strength of an energetic material is its heat of formation (ΔH_f). The higher the value of ΔH_f, the more energy is available to be released.

Energetic materials can be composed of an oxidizer and a fuel source. Once the proper stimulus is applied, the oxidizer and fuel will mix and deflagrate as in a rocket propulsion system. In gun systems it is very challenging to design this two component system to achieve deflagration. Instead, both the oxidizer and fuel are present in the same material and even the same molecules.

Traditionally, to make a molecule energetic, nitroester, nitro, nitramines, and azido groups are added to it as shown in Fig. 2. Besides each group containing at least one nitrogen atom, these groups also share another commonality: they all have a weak heteroatom bond that can be cleaved to initiate the cascade of reactions leading to energy release. The nitroester O–N bond is quite labile and can undergo rapid homolytic degradation to form oxide and NO_2 radicals. The azido groups undergo decomposition during combustion to form nitrogen gas, hydrogen gas, and a cyanide functional group while releasing 685 kJ/mol [19]. Azides are especially attractive because they have very high heats of formation ($\sim$350 kJ/mol) [20].

Incorporating multiple nitrogen atoms into aromatic rings is another method of making energetic materials as in the case of tetrazoles and tetrazines.

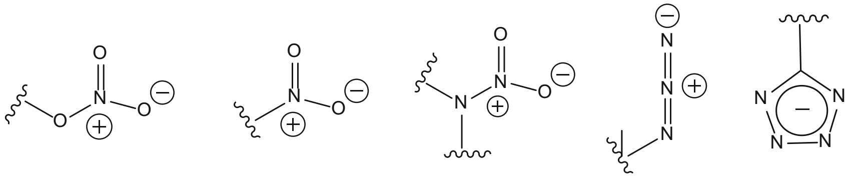

nitroester **nitro** **nitramine** **azido** **tetrazole**

The typical gun propellant is comprised of a combination of energetic materials to achieve its desired function. Energetics for gun propellants are in essence controlled gas generators and should deflagrate, not detonate. Ideal gun propellants burn to completion, leaving no residue, and generate small molecular weight gases such as N_2, CO_2, CO, and H_2O. These gases, through their motion, bombard the projectile and generate the pressure that propels the projectile out of the gun barrel.

4.2 Energetic Binders

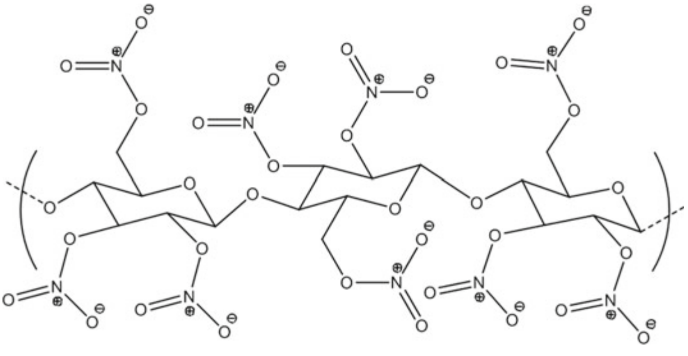

Nitrocellulose

Traditionally, a gun propellant consisting solely of the energetic binder nitrocellulose has been called a single base propellant. The polymeric nature of this binder allows the material to be extruded into any desirable configuration and maintain its shape. The predominant binder in single base and all gun propellants is nitrocellulose (NC). Currently fielded single base propellants include AFP-001, and M1.

NC is a nitrated form of cellulose. There are three hydroxyl groups available for nitration, and depending on the reaction conditions various positions get nitrated. Generally, nitration is performed in a mixture of nitric (HNO_3) and sulfuric acids (H_2SO_4). At HNO_3 concentrations less than 75% and greater than 82% by weight it has been demonstrated that the nitrocellulose product is perfectly soluble in the reaction medium and this is termed homogeneous nitration [21]. The mechanism of homogeneous nitration proceeds in a stepwise manner as shown in scheme 1. In this case, the relative equilibrium constant for the nitration (K_n) is indicated for each free hydroxyl group. The hydroxyl of cellulose at position six has the highest K_n of 30 and is most likely to undergo the first nitration reaction, while the hydroxyl at position 3 has the lowest K_n. The mono-nitrated cellulose will then undergo subsequent nitration to the di-nitrated and finally tri-nitrated NC polymer. Sparse

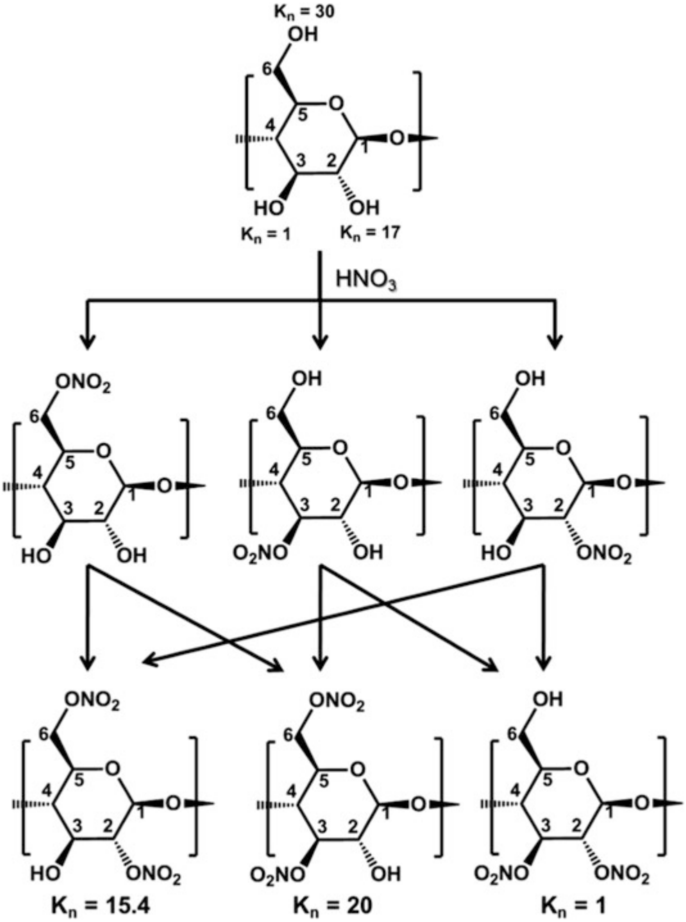

Scheme 1 Formation of nitration products of cellulose

amounts of the 2, 3 dinitrated products are formed [22]. Homogeneous nitration is not employed to make military grade NC, owing to the fact that the presence of water in the reaction mixture severely hampers nitration.

Heterogeneous nitration is performed at HNO_3 concentrations between 75 and 82% by weight. In this case, the NC is an undissolved solid in solution. This may at first appear counterintuitive as to why higher nitration levels are achieved in a molecule that is not fully dissolved, but it has been demonstrated that water diffuses less into the solid NC than does the HNO_3. Therefore, the free hydroxyl groups have higher local concentrations of acid in the heterogeneous process [23]. It was demonstrated via [13] C-nuclear magnetic resonance analyses that in heterogeneous nitration, the free hydroxyl at position 6 of cellulose is exclusively nitrated in the initial step [24]. Only subsequent nitrations occur at the 2 and 3 positions of the polymer.

Other important aspects of the properties of NC are determined by the source of cellulose. Cellulose can be obtained from wood pulp or cotton linters. The source greatly affects the mechanical properties of NC, which in turn effects its ballistic performance. Recently, a group examined NC made from bacterial cellulose. Bacterial cellulose is composed of ribbon-like microfibrils that are two orders of magnitude smaller than plant cellulose. They demonstrated that thermally it behaves the same as conventional NC, but owing to its differing physical properties, it may exhibit altered performance ballistically [25].

A variant of NC, cellulose acetate nitrate (CAN), was also recently examined in gun propellants. In this case, any free hydroxyl groups on NC were acetylated. This was performed in efforts to reduce the sensitivity of the material, however the addition of the non-energetic acetate groups also leads to a reduction in available energy. It was demonstrated in a 105 mm howitzer that although a CAN based propellant formulation was able to perform similar ballistically to the standard M67 propellant, the CAN propellant fared worse in a fragment impact test. It was proposed that the more severe response to fragment impact was due to the higher burn rate of the CAN propellant causing over-pressurization before the deflagrating propellant could vent through the holes caused by the fragment [26].

Recently, the functionalization of cellulose with energetic groups other than nitrate esters was performed in various efforts to produce an energetic polymer with material properties similar to those of NC, yet with more long term stability. It was demonstrated via variable heating rate differential scanning calorimetry (DSC) experiments that the thermal stability of the azidodeoxy cellulose (AZDC) was greater than CAN, which was greater than azidodeoxy cellulose nitrate (AZDCN) [27]. Nitramine functionalized variations of cellulose have also been synthesized. Butylnitraminocellulose (BNAC) and methylnitraminocellulose (MNAC) were synthesized and mixed with aminodinitramide (ADN). BNAC and

MNAC propellants were found to outperform NC at binder concentrations below 50% by weight [28].

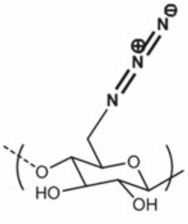

AZDC

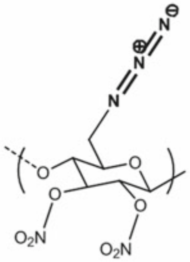

AZDCN

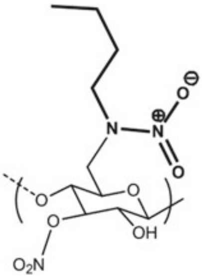

BNAC

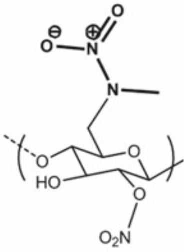

MNAC

4.3 Energetic Plasticizers

Another common component of propellant formulations are energetic plasticizers that make the material easier to form into various shapes and allow for some mobility of materials within a propellant grain. Plasticizers function by intercalating themselves between the polymer chains and disrupting the weak van der Waals and hydrogen bonding interactions that hold the polymer chains tightly together. This intercalation is caused by the plasticizer in essence solvating the polymer and swelling the material, thusly also increasing the void volumes between polymer chains. Since plasticizers are usually small molecules, once intercalated, they permit the polymer chains to twist and glide, thus acting as a lubricant. All of these interactions between the energetic polymers and plasticizers are aimed at lowering the glass transition temperature (T_g) of the material. The glass transition temperature is the temperature below which the components of an amorphous material such as a gun propellant have no motility causing the material to become very brittle. Brittleness is detrimental towards proper ballistic performance, since a brittle propellant breaks up into many fragments during the ballistic cycle thus increasing the available surface area for combustion. As can be inferred, the plasticizer's melting point correlates to how low the T_g of the resultant material will be.

Plasticizers improve the mechanical properties of propellants. One test to evaluate these mechanical properties is via uniaxial compression. This test simulates the types of compressive forces that the propellant grains would experience during the ballistic cycle by being thrown into other grains and the chamber walls. A typical uniaxial compression result is presented in Fig. 4. In Fig. 4a, a viscoelastic propellant is examined. Initially it undergoes an elastic compression up until the yield point and the slope of that line is the Compressive Modulus (Young's Modulus). The material then work hardens (deforms) up to the failure point, after which the

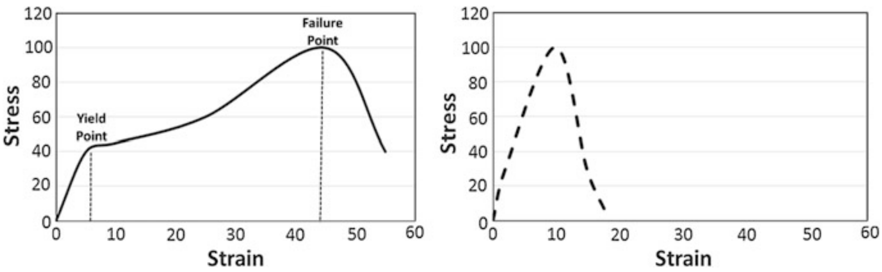

Fig. 4 Typical stress-strain profiles for a (**a**) viscoelastic material and (**b**) Brittle material

material loses all integrity. In a brittle material as presented in Fig. 4b, there is no yield point or work hardening. The material quickly reaches a failure point and loses all integrity.

Propellants consisting of an energetic binder and energetic plasticizer are dubbed double base propellants. Historically, double base propellants consist of nitrocellulose as the binder and nitroglycerin as the energetic plasticizer [29]. The energetic plasticizer is critical to keep the propellant grains from fracturing during the ballistic cycle by improving the Young's modulus for the grains and its ability to work harden and resist fracture due to stress and strain. If the grains fracture, there is a sudden increase in available surface area for deflagration which causes a sudden jump in pressure inside the gun. This could be detrimental ballistically and lead to catastrophic failure of the gun [30]. Currently fielded double base propellants include M9 and JA2.

Recently, JA2, a viscoelastic highly energetic propellant, was examined and its Young's modulus, stress at failure, and strain at failure were determined at 10° intervals from −50 to +80 °C. It was demonstrated that at temperatures below 60 °C, elastic behavior was followed by work hardening prior to material failure. Above 60 °C no elastic region was identifiable. SEM analysis of samples just below the failure strain demonstrated that above 20 °C, the flow in the orthogonal direction relative to the compression was evident due to decreasing microvoid formation. Below 20 °C, microvoid formation and crack tip propagation were the primary failure modes [31].

A variation on uniaxial compression was recently developed by Zhang et al. [32]. In a traditional uniaxial compression test, right cylindrical grains are compressed along their lengths. The grains experience forces only on their circular faces and the sides of the grain are free to expand in the direction perpendicular to the compressive force. In Zhang's apparatus, a large double base propellant grain was pressurized from all sides via the addition of pressurized hydraulic oil inside the chamber, and then underwent uniaxial compression, at various oil pressures. As the oil pressure surrounding the grain increased so did the yield point. Grain fracturing was not observed at higher confining pressures. Also, failure of the grain was shown to occur beyond the limits of the apparatus. Basically, the grain was forced to maintain its shape due to the oil. This may be a better representative test of what is occurring inside a gun chamber during rapid pressurization. The pressure may not be allowing the grains to deform as much as they do in a standard uniaxial compression tester.

The most common energetic plasticizer is nitroglycerin (NG). It is simply the nitrated form of glycerol. This material is highly energetic and extremely sensitive towards any type of stimuli. However, when this material is mixed with NC, there is a synergistic effect in terms of sensitivity. The resulting double base propellant becomes significantly less sensitive than either of the neat materials. A significant concern with double base propellants having a high NG concentration is that the NG migrates over time owing to its small size and structural similarity to NC [33]. It has been known to even seep out of the grain and condense on the surface. In such cases, it makes the propellant very sensitive. Recently, isothermal thermogravimetric analysis (TGA) revealed how readily NG evaporates from the propellant grain at elevated temperatures. Furthermore, like all nitrate esters, NG undergoes catalytic decomposition, which requires the addition of stabilizers to quench these reactions [34]. Many of these properties may be attributed to the NG existing as fine droplets instead of well dispersed molecules in the NC matrix [35]. Below are some nitrate ester plasticizers that have historically been employed as energetic plasticizers which owing to their similarity to NG share the same benefits and drawbacks to varying degrees. Recently, a propellant consisting of 60% NC, 28% NG, and 9.5% TEGDN prepared by a solventless extrusion technique was analyzed for its safety and thermal stability. It was shown that this well plasticized propellant's thermal characteristics were mainly governed by NC's thermodynamic behavior [36].

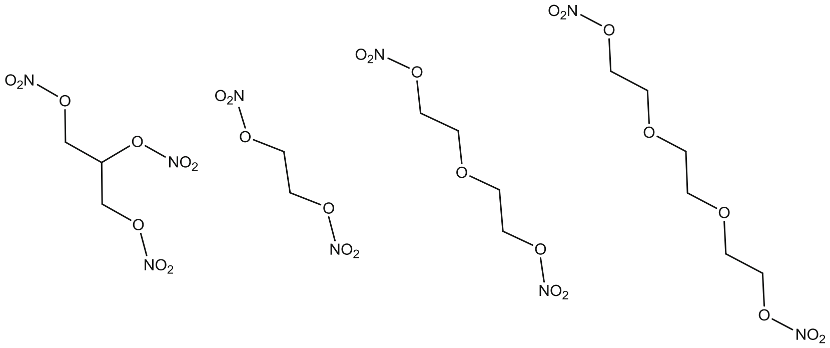

Nitroglycerin (NG)

Ethyleneglycol dinitrate (EGDN)

Diethyleneglycol dinitrate (DEGDN)

Triethyleneglycol dinitrate (TEGDN)

More recent plasticizers for gun propellants include bis-dinitro-propyl acetal/formyl (BDNPA/F), and a variety of nitrooxyethyl nitramines (NENA). BDNPA/F is a eutectic mixture of BDNPA and BDNPF. BDNPF is a solid which is soluble in BDNPA, a liquid. Together they successfully lower the glass transition temperature of the propellant and are quite energetic yet stable owing to the geminal

Table 2 Properties of various NENA derivatives

Properties	Me-NENA	Et-NENA	Pr-NENA	Bu-NENA
Density (g/cm^3)	1.53	1.32	1.26	1.21
m.p. (°C)	38–40	1–5	−2	−27 to −28
DSC exotherm (°C)	218	210	210	210
ΔH_f (kJ/mol)	1113	784	503	259

dinitro groups present. The NENAs utilize both nitramines and nitroesters as sources of their energy. They have been demonstrated to enable propellants to exhibit high burn rates yet retain low flame temperatures. They all have highly positive ΔH_f's. One disadvantage of NENAs with R groups shorter than a butyl functionality, is their melting temperatures are above −2 °C and increase as the alkyl chain shortens (as shown in Table 2), which in turn would raise the T_g of the propellant formulation. Sadly, the ΔH_f follows the opposite trend with butyl-NENA having the lowest value (259 kJ/mol), yet they are all positive [37]. Thusly, butyl-NENA has been shown to improve the energy content, insensitivity, and mechanical properties in single, double, and triple base propellant formulations [38].

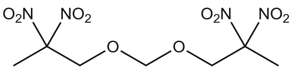

BDNPF

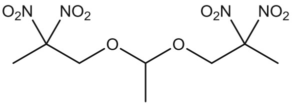

BDNPA

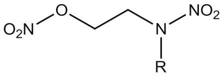

NENA

Recently, Yan's group examined 10 nitrate ester plasticizers as shown in Fig. 5, to determine their thermal stabilities and correlate them to structural motifs [39]. They determined that each nitrate ester undergoes the same decomposition mechanism beginning with homolytic cleavage of the O–NO_2 nitroester bond with a bond dissociation energy on the order of 150 kJ/mol. Three exceptions to this trend were NG, TMPTN, and TMETN which exhibited significantly lower decomposition activation energies of 100 kJ/mol owing to their tendency to evaporate. They also demonstrated that in these nitrate esters a general trend towards improved thermal stability was the placement of nitromethyl groups (–CH_2–ONO_2) at tertiary carbons, followed by nitro groups (–NO_2), and lastly methyl groups (–CH_3).

Another plasticizer that has garnered some interest over the past few years is Dinitro-diaza-alkane (DNDA 57). This is a mixture of three linear nitramines, 2,4-dinitro-2,4-diazapentane (DNDA-5), 2,4-dinitro-2,4-diazahexane (DNDA-6), and 3,5-dinitro-3,5-diazaheptane (DNDA-7). Propellants that utilize it have exhibited the ability to have flat temperature profiles [40]. Traditionally, propellants exhibit lower muzzle energies at colder temperatures. Thusly, at cold temperatures, muzzle velocity and range in gun systems is reduced. A good deal of effort has been placed in improving cold temperature performance especially via plasticizers.

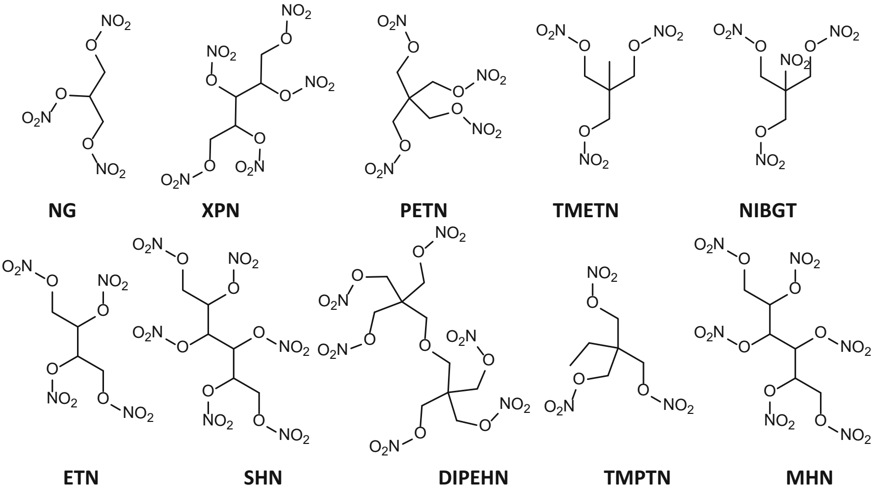

Fig. 5 Series of Nitroesters examined by Yan for thermal stability/structural relationships

The three components of DNDA 57 were individually synthesized and their fragmentation patterns determined by gas chromatography coupled with mass spectrometry in both electron impact and chemical ionization modes. They were shown to all fragment in the same pattern with the first fragment forming via cleavage between the two nitramine groups. The DNDA mixture was demonstrated to have excellent small scale sensitivity properties with an impact sensitivity of 170 cm (RDX is 42 cm), and a frictional sensitivity of 36 kg (RDX is 16 kg). Furthermore, through analysis of viscosity, it was demonstrated that for the energetic binder poly glycidyl nitrate, DNDA 57 is a significantly better plasticizer than BDNPA/F [41]. BDNPA/F as discussed previously is a good plasticizer but is very difficult to produce at large scales. DNDA 57 is much easier to produce at large scales.

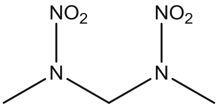

DNDA 5

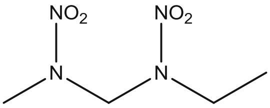

DNDA 6

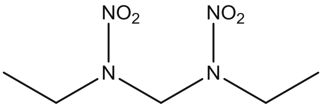

DNDA7

Recently, energetic plasticizers containing azide functional groups have been synthesized and examined. Propellants containing bis[2-azido-1-(azidomethyl)ethyl]malonate (AMEM) and bis[2-azido-1-(azidomethyl)ethyl]glutarate (AMEG) plasticizers were produced and exhibited good ballistic properties [42]. Another azido plasticizer, 1,3-diazido-2-ethyl-2-nitropropane (AENP), was synthesized in three steps from nitropropane. This plasticizer had an energy output of around 2000 J/g, a low glass transition temperature of −96.8° C, and significantly lowered the viscosities of the formulations during processing with azido binders such as GAP, BAMMO, and polyNIMMO thereby producing homogeneous mixtures [43].

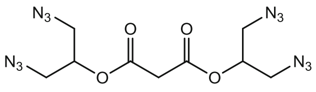

AMEM

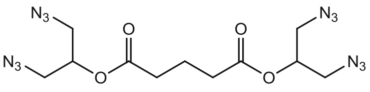

AMEG

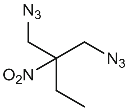

AENP

Two other promising azido plasticizers, 1,3-Bis (azido acetoxy)-2-azido acetoxy methyl-2-ethyl propane (TAAMP) and 1,3-Bis (azido acetoxy)-2,2-bis(azido methyl) propane (BABAMP), were thoroughly evaluated in small quantities [44]. Both of these plasticizers were demonstrated to be quite insensitive towards impact and friction stimuli, yet were quite energetic. However, when these plasticizers were incorporated into a propellant at small percentages (1–2%), there was a slight worsening of the overall propellants response towards impact and friction stimuli. This was not surprising, since these energetic plasticizers were used to replace an inert plasticizer, dibutyl phthalate, thus making the overall formulation more energetic. The ΔH_f of TAAMP and BABAMP were −157.5 kJ/mol and 605.6 kJ/mol, respectively. The very high and positive ΔH_f of BABAMP makes it an attractive plasticizer for high energy propellant formulations and warrants further examination of their effects on mechanical properties and cold temperature performance.

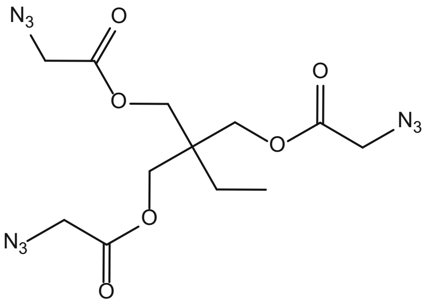

TAAMP

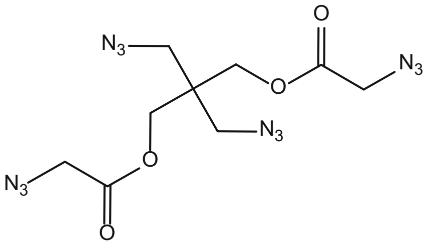

BABAMP

4.4 Energetic Fillers

Another common procedure when formulating propellants is to add a solid energetic filler to double base propellants. Thusly, propellants containing a binder (traditionally NC), plasticizer (traditionally NG), and an energetic filler (traditionally nitroguanidine) are called triple base propellants. Nitroguanidine is an energetic molecule that acts as a flame temperature reducer. Flame temperature reduction is necessary for large caliber applications in order to reduce barrel erosion, since higher flame temperatures have been demonstrated to be one of the primary contributors to gun barrel erosion. Thusly, most triple base propellants are for large caliber applications and are currently in use in the modular artillery charge system.

Solid fillers have also been incorporated into double base propellants in order to boost the ballistic energy of propellant formulations. High energy nitramines such as hexahydro-1,3,5-trinitro-1,3,5-triazine (RDX) and octahydro-1,3,5,7-tetranitro-1,3,5,7-tetrazocine (HMX) have been added to propellants as fillers in order to eliminate dependence on NG for the energy boost owing to NGs stability and migratory issues. In comparison to other fillers examined, such as nitro and azido derivatives, the nitramines possess a higher density, better thermal stability, and positive heats of formation. In the case of HMX as a filler, it has been demonstrated that below 10 MPa, the burning rate of the propellant is controlled by the binder or by binder-nitramine interactions, rather than by the burning rates of HMX itself, but its cost makes it prohibitive to use in gun propellants [45]. RDX has been employed extensively in developmental gun propellants, but its toxicity is an issue [46].

Since these energetic materials are solids, and their incorporation into propellant formulations generally involves the use of solvents in which they are insoluble, their morphology is critical for processability and sensitivity. It has been demonstrated that spherical particles fare better than their non-spherical variants by orders of magnitude in sensitivity tests such as impact and friction. In the case of HMX, it was recently demonstrated that smaller particle sizes lead to improved thermal conductivity, reducing the likelihood hot spot formation, and the resultant sensitivity towards mechanical stimuli such as impact and friction [47]. Attaining the proper morphology of these energetic fillers is critical. Recently, spherical 3-nitro-1,2,4-triazol-5-one (NTO) was produced via crystallization in a variety of particle sizes. It was demonstrated that the particle size was controllable via modification of the cooling and stir rates of the solution (water: N-methyl-2-pyrolidone) [48].

Recently, two nitrate ester solid fillers, erythritol tetranitrate (ETN) and 1,4-dinitrato-2,3-dinitro-2,3bis(nitratomethylene) butane (DNTN), were synthesized and analyzed as shown in Table 3 [49]. It was demonstrated that in comparison to PETN the materials have a more positive oxygen balance and higher heats of formation. However, the heats of formation are less than that of RDX. One other barrier to their use as gun propellant ingredients are the low melting point temperatures of ETN and DNTN. It would appear that based on their oxygen balances and heats of formation, ETN and DNTN are better solid energetic fillers than PETN, but not RDX.

Table 3 Comparison of nitrate ester fillers to RDX

Structure	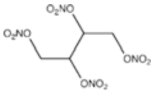	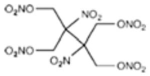	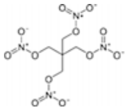	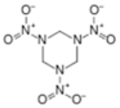
Name	ETN	DNTN	PETN	RDX
Molecular Formula	$C_4H_6N_4O_{12}$	$C_6H_8N_6O_{16}$	$C_5H_8N_4O_{12}$	$C_3H_6N_6O_6$
ΔH_f (KJ/mol)	−474.8	−371	−538.48	−70
m.p. (^oC)	61	85–86	143	204
MW	302.11	420.16	316.14	222.11
OB_{CO_2}	5.29	0	−10.12	−21.61
OB_{CO}	26.48	22.85	15.18	0

4.4.1 High Nitrogen Content (HNC) Energetic Materials and Polynitrogen

High nitrogen content (HNC) materials were designed to contain many nitrogen atoms bonded to one another via single and double bonds. The bond energy of a N–N single bond is 38 kcal/mol, N-N double bond is 100 kcal/mol, and the N–N triple bond is 226 kcal/mol. Therefore, during combustion, nitrogen wants to form triply bonded nitrogen. Because of this drastic increase in bond energy, HNCs release a lot of energy during combustion owing to their large positive ΔH_f.

One of the first HNC compounds was 3-nitro-1,2,4-triazole-5-one (NTO). It was synthesized in 1905, but its demonstration as an energetic material came 80 years later [50]. This molecule had only two carbons. It was demonstrated that NTO had very low shock sensitivity, but good explosive properties. Later HNCs would utilize nitrogen rich heterocycles as their building blocks in order to reduce the amount of hydrogen present. Tetrazoles, such as triaminoguanidinium azotetrazolate (TAGzT), are materials with a lot of energy, and few carbon atoms [51]. TAGzT has been demonstrated to increase the burning rates of a variety of gun propellants especially those containing RDX over a wide pressure range [52]. This was achieved due to the exothermic decomposition of the azotetrazolate in the foam layer, and from fast gas-phase reactions between triaminoguanidine decomposition products, such as hydrazine, interacting with the decomposition products of the RDX [53].

Tetrazole was utilized extensively because of how easy it was to synthesize via click chemistry. In these reactions organic azides are readily reacted with organic cyanides in the presence of a copper catalyst to generate tetrazoles in excellent yields and at low temperatures [54]. Tetrazines have also been coupled to tetrazoles as in the case of 3,6-bis(1H-1,2,3,4-tetrazol-5-amino)-s-tetrazine (BTATz). It has been demonstrated that in the case of hydroxylammonium 3-dinitromethanide-1,2,4-triazolone, which is the salt readily prepared from 3-dinitromethyl-1,2,4-triazolone as

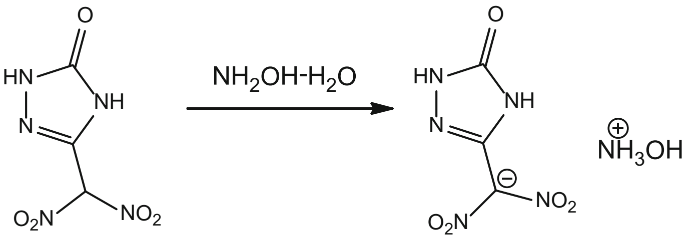

Scheme 2 Synthesis of hydroxylammonium 3-dinitromethanide-1,2,4-triazolone

in scheme 2, π-stacking and extensive hydrogen bonding leads to reduced friction and impact sensitivities even in relation to the uncharged starting material [55].

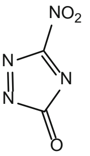

NTO

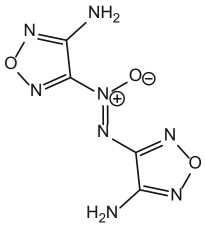

DAAF

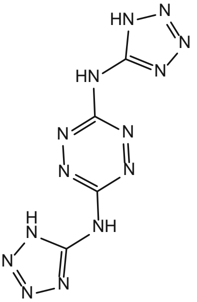

BTATz

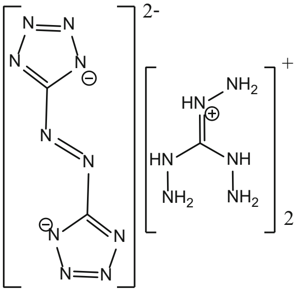

TAGzT

Recent work on the mechanism of combustion involving triaminoguanidinium (TAG) nitrate has demonstrated that TAG acts as an additional heat source for the rest of the propellant owing to its lower thermal stability in comparison to other propellant fillers that are usually present such as ammonium nitrate, and RDX. Kinetic data also demonstrated that the heat generation of TAG combustion is kinetically faster than the heat generation from the combustion of AN or RDX [56]. Basically, TAG compounds burn faster and release more heat which in turn allows other materials such as AN and RDX to combust.

Recently, the effects of the aminoguanidinium counter-cation were examined for their effects on burn rate. Three tetranitrobiimidazolate salts were prepared containing monoamino (aTNBA), diamino (dTNBA), and triamino (tTNBA) guanidinium counter cations [57]. They demonstrated in a strand burner at pressures from 0.2 to 8.6 MPa, that as the guanidinium becomes more functionalized with amino groups, the burn rate increases while the pressure exponent decreases, allowing propellant designers to tailor their burn rates by simply choosing which aminoguanidine to incorporate. This occurs because the density of the material remains relatively unchanged, but the energy of the molecules increase as the degree of amino substitutions increase. Thus the molecules became more energetic per unit density and are able to produce more gas. Recently, two tetranitrobiimidazolate salts containining diammonium and bishydrazinium counter cations were synthesized. They exhibited high densities, positive heats of formation, and were fairly insensitive towards impact and friction [58].

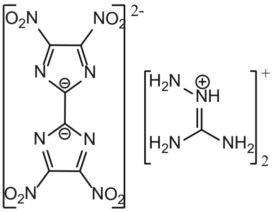

aTNBA

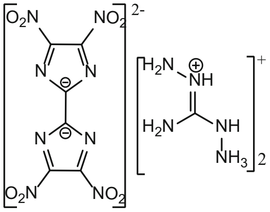

dTNBA

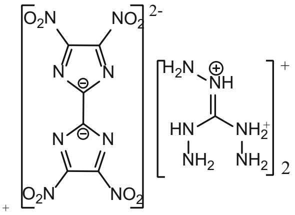

tTNBA

Other counter cations recently examined include 5-aminotetrazolium (ATZ) and 2,4,6-triamino-s-triazinium (TATZ). Both compounds are significantly less sensitive than RDX and neither is capable of detonating due to shock. However, TAGzT has been detonated under similar conditions. The only drawback is that the TATZ does exhibit some electrical sensitivity [59].

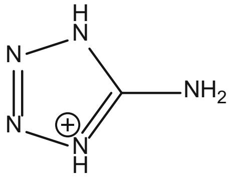

ATZ

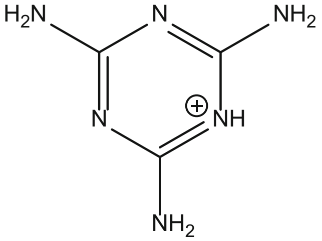

TATZ

Similarly, the energetic salts of 5-oxotetrazole (OTz), were examined for their properties with various counter cations [60]. Traditionally, oxotetrazole derivatives have provided significant energy content, but their sensitivities are very high. As shown in Table 4, a series of guanidine salts and short amines were examined. There is a trend in the first group consisting of guanidinium-5-oxotetrazolate (gOTz), aminoguanidinium-5-oxotetrazolate (agOTz), diaminoguanidinium-5-oxotetrazolate (dgOTz), and triaminoguanidinium-5-oxotetrazolate (tgOTz), that as the counter-cation increases in size by the addition of amine groups the OB becomes less negative, the heat of formation becomes significantly more positive, and the melting point of the materials increase. All of the salts in this group are insensitive towards impact, friction, electrostatic discharge (ESD), with the exception of tgOTz. This data contradicts the general trend in terms of melting point and sensitivities of energetic molecules, which may be due to the addition of another amine moiety to the cation not contributing to an increase in hydrogen bonding with the OTz as evidenced by the crystal structures of the salts. The second group consisting of short amine

Table 4 Properties of OTz salts

Anion	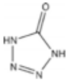	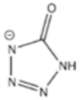						
Cation		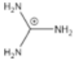	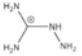	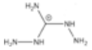	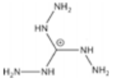	$NH_4^{\oplus}$	$\overset{\oplus}{H_3N}—NH_2$	$\overset{\oplus}{H_3N}—OH\ {}^{*}NH_3O$
Name	OTz	gOTz	agOTz	dgOTz	tgOTz	aOTz	hOTz	haOTz
Mol. formula	CH_2N_4O	$C_2H_7N_7O$	$C_2H_8N_8O$	$C_2H_9N_9O$	$C_2H_{10}N_{10}O$	CH_5N_5O	CH_6N_6O	$CH_8N_6O_3$
MW	86.05	145.12	160.13	175.15	190.16	103.08	118.09	152.11
OB_{CO_2}	−37.18	−71.66	−69.93	−68.51	−67.30	−54.32	−54.19	−31.55
OB_{CO}	−18.59	−49.61	−49.95	−50.24	−50.48	−38.80	−40.64	−21.03
%N	65.10	67.56	69.97	71.97	73.65	67.93	71.16	55.24
ΔH_f (kJ/mol)	5	0	116	224	340	16	173	167
Density (g/cm^3)	1.699	1.612	1.587	1.654	1.625	1.618	1.594	1.634
m.p. (°C)	–	132	156	175	171	199	164	–
D.Temp (°C)	239	189	179	190	174	205	195	138
Impact (J)	>40	>40	>40	>40	15	>40	>40	>40
Friction (N)	360	>360	>360	>360	240	>360	>252	>360
ESD (J)	0.6	1	1	0.65	1	1.5	1.5	0.4

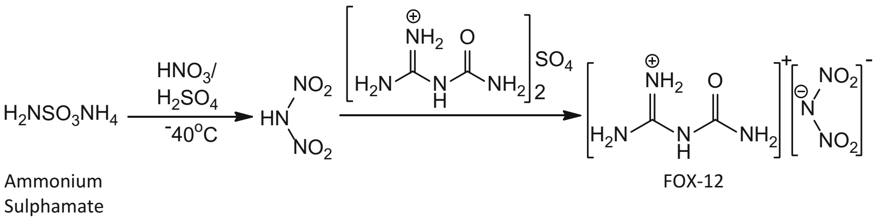

Scheme 3 Revised synthesis of FOX-12

counter-cations included ammonium-5-oxotetrazolate (aOTz), hydrazinium-5-oxotetrazolate (hOTz), and hydroxylammonium-5-oxotetrazolate·NH_3O (haOTz) also exhibited a similar trend regarding the addition of amine moieties to the counter-cation. An identical study examining the guanidinium, aminoguanidinium, and hydroxylammonium salts of 2-nitrimino-5,6-dinitrobenzimidazole was performed and demonstrated similar trends and magnitudes of heats of formation [61].

Guanylurea dinitramide (GUDN or FOX-12) has been known for several years to be an excellent energetic filler for gun propellants owing to its low impact sensitivity, low frictional sensitivity, high thermal stability, and low flame temperature [62]. A hindrance to its utilization in gun propellants has been its high cost. To alleviate this, the yield of the final step in the synthesis of FOX-12 was recently optimized to 50% by lowering the reaction temperature to −40 °C and utilizing a nitrating mixture consisting of concentrated H_2SO_4/HNO_3 at a 1:3 ratio as shown in Scheme 3 [63].

4.4.2 Nanomaterials

By controlling the size and morphology of energetic materials, the sensitivity and burn rates of formulations can be significantly enhanced. Nanomaterials promise to do this. Since nanoparticles have a much larger surface area available for deflagration than do their micron sized counterparts, it is evident that they provide a substantial increase in propellant burn rate. Sensitivity in micron sized materials is due in large part to defects in the crystalline structures that lead to hot spot formation during stress. Nanoparticles have fewer of these defects and are thus less sensitive [64]. However, the validity of certain energetic sensitivity tests such as the BAM friction test has been called into question owing to the experimental setup utilizing sandpaper with micron sized grooves into which the nanometer sized particles can be pushed into during friction tests, thus avoiding the full effect of the frictional forces being applied, and under estimating their true frictional sensitivity [65]. Nano RDX and ammonium nitrate powders pressed pellets were shown to burn faster at elevated pressures than samples made of micrometer-sized particles [66]. It has been shown that thermodynamic properties are dependent upon particle size. As the surface area-to-volume ratio of a particle increases, the particle melting temperature, heat capacity and thermal stability can decrease [67].

RDX, HMX, and CL-20 particles have been produced at the nanometer scales by various methods, including ball milling [68], the rapid expansion of supercritical solutions (RESS) [69], the sol-gel method [70], and solvent-nonsolvent recrystallization [71]. Each of these technique produces nanoparticles, but of varying sizes, thus making comparisons difficult between them since it has been demonstrated that a 200 nm particle is significantly more susceptible to impact threats, than the larger 500 nm particle when both were prepared by the RESS method [72]. The type of methodology employed to make the nanoparticles is also important towards their sensitivity. When nanoRDX was prepared via milling it had an impact sensitivity height of 54 cm, while RESS prepared nanoRDX had an impact height of 75 cm. Raw micron sized RDX had an impact height of 23 cm [73].

Many nanomaterials that are formed, are quite susceptible to agglomeration owing to their increased surface area. One methodology to prevent agglomeration, similar to passivation of metallic nano-particles, is to coat or embed the nano-particles. One group used RESS produced nano-particles and coated them with several polymers. These polymers prevented the agglomeration of the nanoparticles immediately after their formation, and for a year afterwards. This produced very small RDX particles with an average size of 30 nm [74]. Similarly, spray drying produced micron sized particles with nanoRDX dispersed in a polymeric matrix [75].

One recent effort utilized solvent-nonslovent recrystallization with the ionic liquid 1-hexyl-3-methyl-imidazolium bromide as the solvent for nanoHMX formation. They were able to produce spherical and polyhedral particles ranging from 40 to 140 nm in diameter. X-ray diffraction demonstrated that the HMX is in the beta form just like micron sized HMX. The impact sensitivity of the nanoHMX was dramatically increased from an average of 21 to 47 cm drop height. Differential scanning calorimetry (DSC) at heating rates of 5, 10 and 20 °C/min permitted the calculation of the activation energy (E_a) for thermal decomposition of the HMX. This demonstrated that the nanoHMX had a 50 kJ/mol lower E_a than the micron sized HMX [76], indicating that the nanoHMX is more susceptible to thermal threats than micron sized HMX. This is readily explained by nanoparticles having a significantly higher surface area and smaller size than micron sized particle, permitting the nano-particles to absorb heat more rapidly and disperse it throughout their bulk.

NC was also produced as nano-sized spheres by dissolving the NC in a dimethyl formamide solvent at a concentration below 30 mg/mL. Evaporating the solvent at 5 °C produced spheres of NC that ranged from 200 to 900 nm. These particles exhibited a 350% increase in burn rate and a more complete combustion than micron sized particles prepared in a similar manner [77].

Current efforts are also focused on scaling up the production of these nano-materials. Spray drying of RDX has been quite effective at this. RDX nanoparticles are produced inside a polymeric matrix [78]. It has been demonstrated that for RDX, as the particle size distribution decreases, so does its sensitivity to impact stresses [79]. Spray drying has also been employed to form nanocomposite materials from HMX and estane, a polyurethane binder. It was demonstrated that the activation energy of the material improved by 40 kJ/mol, and the average drop height sensitivity was raised by 57 cm in an ERL type 12 apparatus in comparison to raw HMX [80].

4.4.3 Co-crystalization

Co crystallization is a new approach to producing energetic materials. This technology also allows the manipulation of the materials density, thermal stability, and mechanical properties. In this case, a known energetic molecule is crystallized with another energetic or inert molecule. Crystal packing is achieved through non-covalent interactions between the two molecules. This is governed by H-bonding, π–π interactions of aromatic rings, and electrostatic interactions. Hydrogen bonding in energetic materials occurs primarily through the nitro groups as shown in Fig. 6. It has also been demonstrated that nitro groups can rotate out of plane and interact with the delocalized electron cloud of an aromatic ring to form a nitro–π interaction, which have a stabilizing energy between 10 and 52 kJ/mol [81]. This stabilization energy had a direct relationship to the molecules impact sensitivity [82]. The lack of variety in nitro containing energetic molecules to form intermolecular interactions provides some difficulty for engineering energetic co-crystals. Co-crystals should exhibit properties, such as density, energy content, and sensitivity that are quite different than if the two molecules were just blended together in a mixer.

One of the first directed co-crystallization efforts involved the co-crystallization of 2,4,6-trinitrotoluene (TNT) with various inert ingredients. In this case, density and thermal stability of several of the co-crystals were improved, but the use of inert materials did substantially lower the energy content over neat TNT [83]. Furthermore, co-crystallization in these cases involved π-stacking as the primary synthon, which would not be applicable to some of the more conventional high energy materials commonly used in propellants which are not aromatic. Similarly, 2,4,6,8,10,12-hexanitro-2,4,6,8,10,12-hexaazaisowurtzitane (CL-20) was co-crystallized with inert materials but suffered the

Fig. 6 Hydrogen Bonding and nitro–π bonding of Nitro Groups

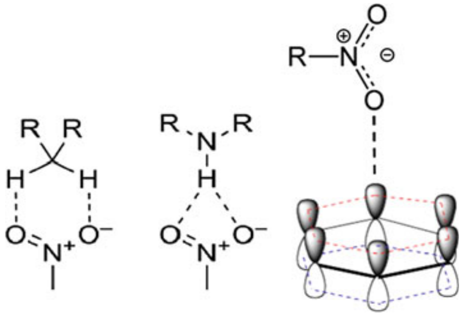

same drawbacks as the TNT effort described above [84]. CL-20 is a known powerful explosive, but has shown some promise as a triple base propellant ingredient. One of its main drawbacks, has been its very high frictional sensitivity [85]. If its sensitivity can be controlled through co-crystallization without a significant sacrifice in energy content, this material could significantly boost propellant output. Recently, porphyrins were co-crystallized with PETN, another explosive compound, from acetone. This was done in order to reduce the sublimation of PETN and improve its stability [86]. HMX was co-crystallized with N-methyl-2-pyrrolidone via a solution evaporation methodology, but other than structural and computational data, no direct information regarding performance or sensitivity was provided [87].

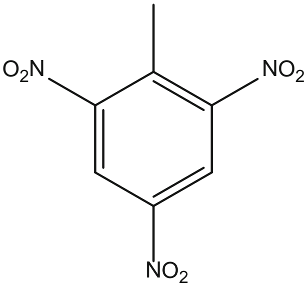

TNT

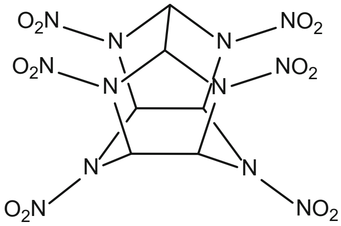

CL-20

The co-crystallization of two energetic materials has also been achieved. TNT has been crystallized with (CL-20) at a 1:1 molar ratio. It was believed that through co-crystallization with another energetic material, the sensitivity properties of CL-20 could be improved without a significant drop in the materials energy content as seen in the cases where CL-20 was co-crystallized with other inert ingredients. Co-crystallization in this case occurred through hydrogen bonding of the nitro groups and aliphatic hydrogens on both molecules. One interesting result was the interaction of several CL-20 nitro groups with the electron deficient ring of TNT, mimicking the nitro–π-interactions observed in other crystals. This CL-20/TNT co-crystal exhibited a density just below that of pure CL-20, but significantly higher than that of TNT. The impact sensitivity based on drop height of an almost 3 kg weight for the CL-20/TNT co-crystal was double that of pure εCL-20. It was demonstrated that upon heating of the co-crystal to above 136 °C, the two components separate and upon cooling do not co-crystallize again [88].

A co-crystal consisting of 2CL-20 moieties and 1 HMX moiety was produced and found to be substantially less sensitive to impact than CL-20 but significantly more brisant than HMX [89]. In a follow on study using the same crystals but prepared via resonant acoustic mixing, it was demonstrated that these crystals were actually more sensitive in an ERL impact test than εCL-20 and just as sensitive in a BAM friction test [90].

A co-crystal of HMX (80%) and TNT (20%) was produced via spray drying. It was demonstrated to be different from the raw materials via scanning electron microscopy, by which the co-crystal had a completely different morphology from either of the individual crystals. X-ray Diffraction demonstrated that it was a unique crystal structure containing both HMX and TNT. Raman spectroscopy demonstrated that the intermolecular interaction is a hydrogen bond between the nitro group of HMX and the hydrogen from the methyl moiety of TNT. DSC confirmed that the co-crystal was different from both a spray dried HMX, raw HMX, raw TNT, and an intimate mixture of HMX and TNT. Impact sensitivity of the co-crystal was shown to be 62.1 cm, while the intimate mixture of the two ingredients was at 31.3 cm, thus indicating that co-crystallization could indeed improve the sensitivity of these materials [91].

A variation of co-crystallization was utilized by Jung in which they employed HMX as a seed for crystallization of NTO. They demonstrated that they were able to generate core-shell particles in which the highly energetic HMX was surrounded by the less sensitive energetic NTO [92]. Similarly, CL-20 was coated with 1,3,5-triamino-2,4,6-trinitrobenzene (TATB) using 2% by weight of an estane polymer as a glue, and the entire CL-20 surface was covered with TATB. The shell thickness varied from 3 to 10 μm, and the material exhibited significantly improved sensitivities towards friction and impact stimuli over the pure and mixed materials [93].

In a surprising turn of events, Qui et al. [94] were able to synthesize nanoparticles of a CL-20/HMX co-crystal. They employed an aqueous bead milling technique on stoichiometric amounts of CL-20 and HMX crystals. After about 1 h, all of the individual crystals of HMX and CL-20 had become co-crystals as confirmed by x-ray diffraction with particles sizes less than 200 nm as confirmed by scanning electron microscopy. Unfortunately, no sensitivity or performance data on these co-crystals have been presented as of yet.

5 Low Weight Percentage Additives

Organic and inorganic ingredients can be added to propellants in small quantities (<4%) for various desired effects. These additives include stabilizers, flash suppressants, opacifiers, burn rate modifiers (e.g. deterrents), and lubricants. In fielded propellant formulations, there may be several additives. For instance, various potassium salts may be present to mitigate flash, and dibutyl phthalate may also be present as a deterrent to control the propellant's burn rate. These low weight percentage additives can be present as either solids or liquids.

If a propellant contains an energetic material with a nitroester bond, then some kind of stabilizers will need to be present. Nitroester bonds, as discussed previously, are very labile with a dissociation energy of the N–O bond being only 150 kcal/mol. Because of this, they undergo spontaneous homolytic cleavage during long term storage. The resulting radicals further damage the remaining energetic materials via auto-catalytic degradation which in turn causes self-heating and can eventually lead to detonation. Stabilizers such as ethyl centralite, diphenylamine, and akardite II react with the various nitro radicals that are produced during long term storage of nitroester containing energetics thus prolonging the propellant's shelf-life. A recent study demonstrated that the relative humidity plays a critical role in stabilizer depletion due to aging, with higher humidities causing less depletion of the stabilizers N-methyl-4-nitroaniline and 2-Nitro-diphenylamine [95]. By employing DSC to calculate the activation energies of decomposition of NC films containing varying amounts of diphenylamine stabilizer, the optimal amount of stabilizer can be determined [96]. Recently, researchers combined computational modeling with experimental evidence to demonstrate that for a series of structurally similar malonanilides as the HOMO-LUMO gap decreases, the stability effect increases [97]. Further study is needed to compare this trend to non-similar structures to determine if it could be a stabilizer design tool.

Recently, the zeolite Clinoptilolite was demonstrated to exhibit stabilizing properties in double base propellants (59% NC:31% NG). According to the Bergmann—Junk test and bomb calorimetry, a sample containing 4.0% by weight of the nano-Clinoptilolite (prepared by mechanical grinding of the micron sized sample) exhibited significantly better performance as a stabilizer than did the centralite present at 3.0% by weight. This stabilization effect is presumed to occur by the attraction of the NO_x to the cationic surface groups on the zeolite. Furthermore, atomic force microscopy of the propellant grain surfaces revealed that the nano-Clinoptilolite containing grains were more homogeneous on their surface [98].

A unique study was recently published wherein three identical propellants were analyzed by DSC to determine their service life. Each double base propellant was identical and utilized methylcentralite (MC) as a stabilizer and dibutylphthalate (DBP) as a surface burn rate modifier (deterrent). The only difference between the propellants was that one was recently produced, one had been in storage for 15 years, and one had been in storage for 25 years. After an exhaustive DSC analysis of the various thermodynamic properties of each propellant it was demonstrated that the unaged propellant after undergoing simulated aging at 65.6 °C for 60 days was identical thermodynamically to the 25 year naturally aged propellant [99]. When they examined the compositions of these propellants they demonstrated that the stabilizer does decrease from 3 to 2.4% during natural aging, but drops to 2.2% during accelerated aging, further indicating that in terms of stabilizer content, accelerated aging is a valid technique for estimating safe shelf-life of a propellant. They also demonstrated that during natural aging, the DBP concentration can drop from 4.9 to 4.0% over 25 years, while accelerated aging for 120 days further decreased the DBP concentration to 3.1%. Similarly, during natural aging, the NG content decreased minimally (around 1%), but under accelerated aging, the NG content diminished by roughly 6%. This loss of plasticizers during natural aging will worsen the mechanical properties, which would be further exacerbated by accelerated aging. This was confirmed by dynamic mechanical analysis (DMA), which demonstrated that the T_g increased from −27 to

−18 °C during natural aging. Accelerated aging produced the opposite trend. Surprisingly, accelerated aging of the fresh propellant first raised the T_g of the propellant, owing to the evaporation of the plasticizers from the propellant, but after 30 days it began to decrease, most probably due to NC chain scission [100].

Carbonaceous materials are extensively used in propellants as opacifiers and flame suppressants. Graphite is used as a surface glaze which reduces the frictional coefficient of propellant grains thus allowing the grains to pack more efficiently in a cartridge and have a higher loading density. But other forms of carbon have other unique effects and properties. When [60] fullerene, a soccer ball-like structure composed of benzene and pentacene substructures, was mixed with HMX at just 1% by weight, the impact sensitivity was improved by 40%, while the friction sensitivity was improved by 30% [101]. This may be due to fullerenes ability to rotate even in the solid state, thus acting like ball bearings in the material and allowing the HMX to slide as if it was lubricated [102]. Carbon nanotubes have also demonstrated their ability to desensitize HMX [103]. More recently, graphene and HMX were shown through molecular modeling to be more stable as a composite material [104].

One of the more unique procedures has been the attempts to encapsulate energetic materials inside of carbon nanotubes. Density Functional Theorem (DFT) modelling by Abou-Rachid's group demonstrated for a variety of energetic materials, that there is a significant stabilizing effect experienced by the energetics within the interior cavity of the nanotube [104]. One group, successfully filled carbon nanotubes with potassium nitrate, as evidenced by DSC, and TEM, via wet chemistry methods, and employed them as a nanoinitiator [105]. One important aspect to consider when employing carbon encapsulation as a means of energy partitioning is that you are severely lowering the oxygen balance of your energetic material since you are adding a lot of carbons to the material.

An interesting variant of graphene, is graphene oxide (GrOx). GrOx is prepared under harsh oxidizing conditions using potassium permanganate and sulfuric acid [106]. GrOx is thermally unstable and undergoes a strong exothermic degradation reaction upon heating [107]. It was recently demonstrated via non-isothermal DSC that that when GrOx was coated onto the surface of HMX crystals at 2% by weight, the activation energy for the decomposition reaction increased by 23.5 kJ/mol. Furthermore, the impact and friction sensitivities were improved by 90 and 70% respectively [108]. It is apparent that the HMX and GrOx synergistically assist one another similar to the way NC and NG mixtures become less sensitive but more energetic.

6 Propellant Formulation Modeling and Design

Before proceeding to the laboratory and starting propellant formulation development, with all of the ingredients discussed so far, some modeling is first required. There are various proprietary thermodynamic codes (TIGER [109], BLAKE [110], CHEETAH [111], EXPLO5, [112] ZNWNI [113], THERMO [114]) currently in use that in essence provide the same information. They utilize the properties of molecules such as heat of formation, molecular formula, and density to provide the propellant developer with some useful initial information on the potential performance of the proposed propellant formulation. Most of these codes provide the impetus, which is the energy of the propellant also known as the propellant force, and the adiabatic flame temperature (T_v) of the propellant at constant volume. In these ideal cases, the impetus is the ability of the propellant to do work on a projectile [115]. Table 5 provides the BLAKE output of an M1 propellant consisting of 83.11% nitrocellulose, 9.77% dinitrotoluene, 4.89% dibutylphthalate, 0.98% diphenylamine, 0.5% water, and 0.75% ethanol [116]. In this case the loading density was varied from 0.2 to 0.3 g/cc. As the loading density increased the T_v increased slightly, while the pressure almost doubled. However, the impetus and the molecular weights of the gasses remained relatively unchanged. These predictions allow for the propellant developer to optimize a formulation before initial processing.

These thermodynamic codes also provide the concentrations of a variety of the combustion products as shown in Table 6. From the combustion products one can immediately approximate how erosive the propellant will be based on the ratios of N_2, H_2, and CO gasses coupled with the flame temperature. Certain gasses such as N_2 will form a protective coating of iron nitride with the gun barrel steel, while others such as H_2 and CO are known to react with the metals present, thus hastening the erosion by forming iron carbide [117]. There is a low activation energy for the

Table 5 Blake Output of M1 propellant

Loading density (g/cc)	T_v (K)	Pressure (MPa)	Impetus (J/g)	Mol. Wt. gas (g/mol)	Co-vol (cc/g)
0.20	2447	236.0	919.2	22.138	1.105
0.25	2454	314.5	919.7	22.188	1.077
0.30	2462	402.4	919.9	22.254	1.048

Table 6 Gaseous output of M1 propellant

Loading density (g/cc)	0.2	0.25	0.3
$CO_{(g)}$	22.94	22.88	22.79
$H_{2(g)}$	9.25	9.11	8.93
$H_2O_{(g)}$	6.09	6.13	6.17
$N_{2(g)}$	4.43	4.41	4.4
$CO_{2(g)}$	2.32	2.33	2.35
$NH_{3(g)}$	0.045	0.062	0.081
$HCN_{(g)}$	0.029	0.042	0.058
$CH_{4(g)}$	0.041	0.073	0.12

All values are in moles of gas per kilogram of propellant dissociation of carbon monoxide on gun steel. Then hydrogen gas present in the propellants combustion products reacts with the oxygen to form water while the carbon diffuses into the gun steel, resulting in surface carburization and a lowering of the melting temperature by several hundred degrees [118]. The presence of a lot of nitrogen gas, especially when using HNC propellant ingredients nitrides the gun steel. This nitride coating prevents the carbon monoxide from reacting with the gun steel, thus reducing erosion [119]. Therefore, a propellant with low amounts of hydrogen and a high N_2:CO ratio is desirable [120].

A recent study determined that these codes tend to under-predict the concentrations of certain toxic gasses such as HCN and NH_3 [121]. In a series of 9MM firings with different propellants it was demonstrated that the concentrations of HCN and NH_3 were found to be orders of magnitude higher than predicted by EXPLO5, when compared to gas analysis performed on the actual gun firings. It was proposed that this increase may be due to more benign propellants having a lower flame temperature which leads to more production of NH_3 and CH_4. These two gasses can then react in the presence of oxygen to form HCN [122]. Reactive force field molecular dynamics (ReaxFF-MD) simulations of the individual components of the formulation, namely, NC, NG, EC, and DPA demonstrated that the major sources for these toxic gasses are the aromatic compounds EC and DPA, not from the nitro groups of NC and NG [123]. As such, these codes may be employed as a design tool to minimize the production of toxic gasses.

Two triple base formulations containing small amounts of TAAMP or BABAMP were likewise analyzed using THERMO. The software was able to predict within 15 J/g the impetus of 5 formulations with varying amounts of energetic plasticizer as validated by closed vessel testing, thus confirming the utility of thermodynamic codes in assisting propellant developers to more efficiently develop propellants [43].

Recently, Son's group demonstrated through Cheetah 6.0 and experimentally that 1,4-dinitrato-2,3-dinitro-2,3bis(nitratomethylene) butane (SMX) mixed with varying amounts of NC can, in terms of impetus, outperform JA2, a benchmark high performance and insensitive gun propellant [124]. Cheetah demonstrated that in a binary formulation consisting solely of NC and SMX, at concentrations of SMX between 35% and 70%, the impetus of the experimental formulation exceeded that of JA2. This implied the potential for SMX to be used as an NG replacement. Surprisingly the addition of 20%DEGDN to the NC/SMX formulation boosted the impetus by over 20 J/g. Normally, the addition of DEGDN to a high energy formulation at the expense of a high energy ingredient such as NG, RDX, or HMX, lowers the impetus, but in this case, the opposite occurred.

7 Processing Effects

Instead of mixing all of the ingredients together in a batch mixer, for safety reasons, there has been a recent push towards infusing the propellant after they have been formed into grains. Single base propellant has been infused with NG after it has been formed into grains and prior to deterring with a polyester. Determination of the concentration profile demonstrated that infusion with NG produced a gradient inside the grain with the lowest concentrations of NG being near the surface and centers of the grain. Their results indicate that the even though the NG was successfully infused into the grain, it also easily moved out of the grain near the surface. This is a common issue with double base propellants containing NG owing to its high mobility through the NC matrix. They demonstrated that after the deterring and infusing the propellant grain exhibited progressive burning while the unaltered base grain was undergoing neutral burning. They also demonstrated that the infused propellant was of higher energy, and produced less erosion by about 16% at a similar chamber pressure [125].

Infusion of NC was also performed with SMX. It was mixed with NC up to a concentration of 40% by weight. Crystals were observed to form on the surfaces of the NC fiber. Subsequent heating above SMX's melting point (~85 °C) caused the SMX to liquefy and penetrate uniformly into the grains. Using this processing methodology a propellant was made consisting of 60%NC and 40%SMX which exhibits impact sensitivity similar to JA2 with a slightly higher friction sensitivity [124]. The increase in friction sensitivity is understandable because while JA2 contains virtually no solid energetic fillers, in this case the researchers added 40% by weight of solids to the formulation.

Consolidated propelling charges are prepared by forming a large charge from smaller propellant grains. In essence, consolidated charges are small propellant grains glued together to form a larger charge. An example of this would be to form a cylinder from small ball powder grains. The benefits of a consolidated charge are the significant increase in the loading density and an inherent progressivity when the consolidated charges break apart into smaller grains, in a process termed deconsolidation. Both of these processes lead to improved ballistic performance [126].

Consolidated charges have been prepared in a variety of ways. In one method, the propellant grains are compressed inside the cartridge case [127]. Another process involves the addition of a solvent, such as acetone, to the propellant grains. Acetone partially solvates the NC causing the grains to swell. These wetted grains are then compacted into the desired charge shape. One drawback to this methodology is that the individual grains do get deformed in the process, altering the ballistics [128]. Yet another methodology employs the coating of propellant grains with a thermally curable binder. These grains were then thermally consolidated into the desired propelling charge shape [129].

Oblate spherical double base propellants plasticized with TEGDN have been consolidated by a combination of techniques. A gelled NC in acetone was utilized as the binder to thermally consolidate the grains. Furthermore, the charge forming tool was coated with an NC/TiO_2 mixture, causing the outermost layer of this consolidated charge to have a deterrent. This combination technique demonstrated significantly improved mechanical properties in terms of uniaxial compression. Both stress and strain increased more than twofold before failing. Closed vessel analysis revealed that the consolidated charge exhibited a two stage combustion event. First the outer NC/TiO_2 coating layer burned away followed by deconsolidation of the charge which lead to a drastic jump in dynamic vivacity [130].

Recently, a combination of processing techniques were employed to improve upon consolidated gun propellants. Researchers prepared seven perforated grains using foaming and compression molding technologies. Through a series of quenched combustion tests, they were able to demonstrate a marked improvement [131] over previous consolidated propellants examined [132]. This was achieved by ensuring that deconsolidation of the propellant grains occurs later in the ballistic cycle which was a major drawback for previous efforts involving consolidated gun propellants.

Foaming of propellants increases the porosity of propellants, thusly increasing the surface area available for combustion which in turn increases the burn rate [133]. One drawback to this is the reduced density of the propellant. For this reason, foamed energetic materials have been primarily examined for combustible cartridge case and case-less ammunition applications. Recently, foaming of a poly-methylmethacrylate (PMMA)—RDX composite was examined. Foaming was achieved via saturation of the propellant in a supercritical CO_2 (scCO_2) fluid under high pressure. The CO_2 penetrates into the propellant and once the pressure is quickly removed the CO_2 evacuates the propellant leaving a porous material. The investigators varied both the RDX content and expansion ratio, which corresponds to porosity via a supercritical CO_2 foaming methodology. They demonstrated that at 55% RDX content the foamed material was equivalent to the existing felted fiber case technology in terms of force constants at 450 J/g. The force constants are the energy content of the material. At higher RDX concentrations (75%) they were able to achieve a force constant of 858 J/g which is getting close to the impetus of certain gun propellants. This is impressive because they employed an inert binder. If they were able to utilize an energetic binder the impetus would dramatically improve. They also demonstrated that as porosity or RDX content increased so did the progressivity of the burning in closed vessel tests. One surprising result was that foaming temperature played virtually no role in the performance of the materials [134].

Then, Yang and co-workers altered their foaming procedure, by adding a timed desorption step to their super-critical CO_2 process. In this case the supercritical CO_2 fluid is allowed to escape from the material for a specified amount of time. This leaves the surface of the propellant with less CO_2 than the core of the propellant. Once it is quenched, the CO_2 gradient that was established forms a material that is porous on the inside and has a significantly less porous skin on the exterior of the grain [135].

Foaming of NC has presented a challenge until a recent process was developed, using supercritical foaming technology which consists of dissolution of gas, cell nucleation, cell growth, followed by stabilization of foam structures [136]. The challenges for NC foaming derive from its high crystallinity. The crystalline regions of NC prevent penetration of the inert gasses commonly employed such as CO_2, thus preventing pore formation [137].

Another recent study examined foamed NC double base propellant containing NG or TEGDN as a plasticizer [138]. These researchers were able to control porosity of the propellant grains and demonstrated via closed vessel testing that as porosity increased, so did gas generation. Furthermore they demonstrated that the presence of plasticizers, NG and TEGDN, improved $scCO_2$ uptake, and subsequent porosity increased. Without plasticizers no differences between foamed and unfoamed propellants were visible during closed vessel testing. Foaming increased the burn rates significantly. The desorption of CO_2 from foamed propellants was fastest for the NG based propellant. TEGDN demonstrated itself to be a better plasticizer for these foamed propellants. Furthermore, they also prepared samples with an outer skin and demonstrated via interrupted combustion testing in a closed vessel that the inner porous cores burn out before the outer skin does [139].

Other studies employed potassium nitrate to generate porosity in single base ball powder grains. They incorporated the potassium nitrate (KNO_3) into the formulation and after formation of the ball powders, they washed the propellant with water. The water dissolved and removed the KNO_3, but left the rest of the propellant untouched thus generating porous ball powder. The porous ball powders were then shaped with acetone or ethyl acetate which eliminated the porosity on the surface of the grains, while leaving the internal porosity intact. This produced ball powders with a fast burning core. Finally the grains were deterred with the standard dibutyl phthalate (DBP) or poly(ethylene glycol dimethacrylate) (PEGDMA) [140]. They demonstrated that the amount of KNO_3 added, and the conditions of the shaping greatly affected the combustion characteristics of the ball powders in closed vessel tests. Furthermore, the PEGDMA was polymerized inside the grain to allow the monomers to disperse into the grain and form a deterrent gradient and produce more progressive combustion than the DBP deterred grains.

Another technique that generated porosity in NC utilized titanium nanoparticles as nucleation sites. Cylindrical propellant grains were made by standard mixing, and extrusion of NC (11.8–12.4% nitrogen) with titanium nanoparticles (20–40 nm diameter). The nano-titanium ranged from 5 to 15% by weight. The cylindrical grains then underwent foaming via immersion in $scCO_2$, and the use of ethyl acetate to partially dissolve/soften the NC and allow the CO_2 to better diffuse into the grain. The titanium acted as nucleation sites for the $scCO_2$ generating NC grains that have some pores filled with nano-titanium. As the concentration of the nano-titanium increased, agglomeration became more pronounced. Also, standard mixing techniques were shown to inadequately mix the nano-titanium, causing some areas of the grain to have significantly higher local concentrations of titanium. These materials were then tested in a closed vessel and their impetus was demonstrated to decrease with increasing titanium content. However, closed vessel testing also demonstrated that the foamed propellant with 10% nano-titanium had the highest burn rate, contradicting the impetus trend observed [13].

8 Summary

Although the traditional role of gun propellants has remained essentially the same, the often competing requirements of advanced weapon systems have necessitated a tremendous amount of effort over past five years, from 2010 to 2015, to develop new binders, plasticizers, and fillers, into high energy insensitive formulations. The majority of the binder work has focused on functionalizing cellulose with non-nitrate ester groups to produce a more stable form of energetic cellulose. A wide variety of novel plasticizers have been examined that exhibit promise in making gun propellant formulations less sensitive to shock and thermal stimuli. The fillers are the broadest category of propellant ingredients, and have had the largest amount of materials examined. Nano-particles, alternate forms of carbon, and energetic co-crystals have been tested as gun propellant ingredients that can boost performance and stability while reducing sensitivity, hygroscopicity, and combustion residue generation. At the propelling charge level, novel techniques such as foaming and consolidating propellant grains promise to improve gas generation behind the projectile later in the ballistic cycle, leading to increases in muzzle energy.

While traditional propellant ingredients consist of a relatively few available and proven materials, recent discovery and manipulations of new molecules are allowing the gun propulsion developer to extend the state of the art in propellant formulations, providing the warfighter with improved capabilities on the battlefield. In the next five years, continued technical advancements in these new ingredients and formulations may lead to a paradigm shift in the development of gun propellants.

References

1. Koc S, Ulas A, Yilmaz NE (2015) Propellants, Explos, Pyrotech 40:735
2. (A) Klingenberg G (1989) Propellants Explos Pyrotech 14:57. (B) Klingenberg G, Heimerl JM (1987) Combust Flame 68:167. (C) Carfagno SP (1961) Handbook on gun flash, report DTIC AD327051. The Franklin Institute, Philadelphia, PA, USA. (D) Yousefian V, May IW, Heimerl JM (1980) 17th JANNAF combustion meeting, Hampton, 22–26 Sept 1980, vol 2, p 124. (E) Heimerl JM, Keller GE, Klingenberg G (1988). In: Stiefel L (ed) Gun propulsion technology. AIAA, Washington D.C., p. 261
3. Bougaev AV, Gerasimov S, Erofeyev VI, Kolchev SV, Mikhailova1 YA (2014) 28th international symposium on Ballistics Atlanta, GA, 22–26 Sept 2014
4. Birk A, Guercio MD, Kinkennon A, Kooker DE, Kaste P (2000) Army research laboratory technical report ARL-TR-2371
5. (A) Hamlin SJ, Beyer RA, Burke GC, Hirlinger JM, Martin J, DL Rhonehouse (2005) Proceedings of SPIE-the international society for optical engineering, p 5871(Optical Technologies for Arming, Safing, Fuzing, and Firing), 587102/1-587102/9. (B) Beyer RA, Hirlinger JM (1999) Army research laboratory technical report ARL-TR-1864. (C) Beyer RA, Boyd JK, Howard SL, Reeves GP (1999) Army research laboratory technical report ARL-TR-1993

6. Xiao Z, Ying S, Xu F (2015) Propellants, Explos, Pyrotech 40:484
7. Sättler A, Åberg D, Rakus D, Heiser R (2014) 128th International symposium on Ballistics, Atlanta, GA, 22–26 Sept 2014
8. Bieles JK (1986) 9th International symposium on Ballistics, Shrivenham, UK, April 29–May 1 1986
9. Nakamura Y, Ishida T, Miura H, Matsuo A (2007) 23rd international symposium on Ballistics, Tarragona, Spain, 16–20 Apr 2007
10. Howard SL (2011) Army research laboratory technical report ARL-TR-5658
11. Baschung B, Bouchama A, Comet M, Boulnois C (2014) 28th international symposium on Ballistics, Atlanta, GA, 22–26 Sept 2014
12. Howard SL, Churaman WA, Currano L (2014) Army research laboratory technical report ARL-TR-6950
13. Su J, Ying S, Xiao Z, Xu F (2013) Propellants, Explos, Pyrotech 38:533
14. Muthurajan H, Ghee AH (2008) Central Eur J Energ Mat 5(3–4):19
15. Zheng W, Chen H, Li Q, Pan R, Lin X (2014) Int J Energ Mat Chem Propul 13:421
16. Harrland A, Johnston IA (2012) Defence science and technology organisation technical report DSTO-TR-2735
17. Leciejewski ZK, Surma Z (2011) Combustion. Explosion, Shock Waves 47:209
18. Pauly G, Scheibel R (2008) 43rd Annual armament systems: gun and missile systems conference & exhibition, New Orleans, LA, USA, 21–25 Apr 2008
19. (A) Kubota N (1988) Propellants Explos Pyrotech 13:172. (B) Kubota N, Sonobe T, Yamamoto A, Shimizu H (1990) J Prop Power 6:686
20. Pant CS, Wagh RM, Nair JK, Gore GM, Venugopalan S (2006) Propellants, Explos, Pyrotech 31:477
21. Miles FD (1955) Cellulose nitrate. Oliver and Boyd, London
22. Rafeev VA, Rubtsov YI, Sorokina TV, Chukanov NV (1999) Russ Chem Bull 48:66
23. Rafeev VA, Rubtsov YI, Sorokina TV (1879) Russ Chem Bull 1996:45
24. (A) Wu TK (1980) Macromolecules 13:74. (B) Chicherov AA, Kuznetsov AV, Kargin YM, Klochkov VV, Marchenko GN, Garifzyanov GG (1990) Polym Sci USSR, Set. A 32:502
25. Sun D-P, Ma B, Zhu C-L, Liu C-S, Yang J-Z (2010) J Energ Mater 28(2):85
26. Manning TG, Wyckoff J, Adam CP, Rozumov E, Klingaman K, Panchal V, Laquidara J, Fair M, Bolognini J, Luhmann K, Velarde S, Knott C, Piraino SM, Boyd K (2014) Defence Technol 10:92
27. Shamsipur M, Pourmortazavi SM, Hajimirsadeghi SS, Atifeh SM (2012) Fuel 95:394
28. Betzler FM, Klapötke TM, Sproll S (2011) Central Eur J Energ Mat 8(3):157–171
29. Nobel A, Armengaud CE (1876) Improvement in gelatinated explosive compounds, US Patent 175, vol 735
30. (A) Ang HG, Pisharath S (2012) Energetic polymers: binders and plasticizers for enhancing performance. Wiley-VCH, Germany. (B) Kumari D, Balakshe R, Banerjee S, Singh H (2012) Rev J Chem 2:240–262
31. Howard SL, Leadore MG, Newberry JE (2015) Army research laboratory technical report ARL-MR-0894
32. Zhang J, Ju Y, Zhou C (2013) Propellants, Explos, Pyrotech 38:351
33. Agrawal JP, Singh H (1993) Propellants, Explos, Pyrotech 18:106
34. Suceska M, Musanic SM, Houra IF (2010) Thermochim Acta 510:9
35. Taylor S, Dontsova K, Bigl S, Richardson C, Lever J, Pitt J, Bradley JP, Walsh M, Šimůnek J (2012) US army engineer research and development center technical report, ERDC/CRREL TR-12-9
36. Yi JH, Zhao FQ, Hu RZ, Xue L, Xu SY (2010) J Energ Mater 28(4):285
37. Simmons RL (1994) NIMIC-S-275-94. NATO, Brussels, Belgium
38. Chakraborthy TK, Raha KC, Omprakash B, Singh A (2004) J Energ Mater 22(1):41
39. Yana QL, Künzela M, Zemana S, Svobodab R, Bartoskovác M (2013) Thermochim Acta 566:137

40. Mueller D (2008) 43rd annual armament systems: gun and missile systems conference & exhibition, New Orleans, LA, USA, 21–25 Apr 2008
41. Vijayalakshmi R, Naik NH, Gore GM, Sikder AK (2015) J Energ Mater 33:1
42. Kumari D, Yamajala KDB, Singh H, Sanghavi RR, Asthana SN, Raju K, Banerjee S (2013) Propellants, Explos, Pyrotech 38:805
43. Ghosh K, Athar J, Pawar S, Polke BG, Sikder AK (2012) J Energ Mater 30(2):107
44. Ghosh K, Pant CS, Sanghavi R, Adhav S, Singh A (2008) J Energ Mater 27:40
45. (A) Zimmer-Galler R (1968) AIAA J 6:2107. (B) Kubota N (1982) 19th Symposium (International) on combustion. The Combustion Institute, USA, Haifa, Israel, 8–13 Aug 1982
46. Parker GA, Reddy G, Major MA (2006) Int J Toxicol 25:373
47. Wang Y, Song X, Song D, Jiang W, Liu H, Li F (2011) Propellants, Explos Pyrotech 36:505
48. Vijayalakshmi R, Radhakrishnan S, Rajendra PS, Girish GM, Arun SK (2012) Part Syst Charact 28:57
49. Oxley JC, Smith JL, Brady JE, Brown AC (2012) Propellants, Explos, Pyrotech 37:24
50. Lee K-Y, Chapman LB, Cobura MD (1987) J Energ Mater 5:27
51. Tremblay M (1965) Can J Chem 43:1230
52. (A) Walsh C, Knott C (2004) 32nd JANNAF propellant explosives development and characterization subcommittee meeting, Seattle, Washington. (B) Mason B, Llyod J, Son S, Tappan B (2009) Int J Energ Mater Chem Propul 8:31. (C) Conner C, Anderson W (2007) 34th JANNAF propellant & explosives development and characterization subcommittee, Reno, Nevada, 13–17 Aug 2007
53. Kumbhakarna N, Thynell S, Chowdhury A, Lin P (2011) Combust Theor Model 15:933
54. (A) Kolb HC, Finn MG, Sharpless KB (2004) Angewandte Chemie international edition 2001 40. (B) Demko ZP, Sharpless KB (2002) Angewandte Chemie International Edition 41:2113
55. Zhang J, Zhang Q, Vo TT, Parrish DA, Shreeve JM (2015) J Am Chem Soc 137:1697
56. Serushkin VV, Sinditskii VP, Egorshev VY, Filatov SA (2013) Propellants, Explos, Pyrotech 38:345
57. Tappan BC, Chavez DE (2015) Propellants, Explos, Pyrotech 40:13
58. Paraskos AJ, Cooke ED, Caflin KC (2015) Propellants, Explos, Pyrotech 40:46
59. Warner KF, Granholm RH (2011) J Energ Mater 29:1
60. Fischer D, Klapotke TM, Stierstorfer J (2012) Propellants, Explos, Pyrotech 37:156
61. Klapotke TM, Preimesser A, Stierstorfer J (2015) Propellants, Explos, Pyrotech 40:60
62. (A) Bottaro JC (1996) Chem Ind 10:249. (B) Bottaro JC, Schmitt RJ, Penwell P, Ross S (1993) Dinitramide salts and method of making same, U.S. Patent 5254324, SRI International, Stanford, CA, USA
63. Badgujar DM, Wagh RM, Pawar SJ, Sikder AK (2014) Propellants, Explos, Pyrotech 39:658
64. Armstrong RW, Ammon HL, Elban WL, Tsai DH (2002) Thermochim Acta 384:303
65. Radacsi N, Bouma RHB, Krabbendam-la Haye ELM, ter Horst JH, Stankiewicz AI, van der Heijden AEDM (2013) Propellants, Explos, Pyrotech 38:761
66. Pivkina A, Ulyanova P, Frolov Y, Zavyalov S, Schoonman J (2004) Propellants, Explos, Pyrotech 29:39
67. (A) Siegel RW (1999) WTEC Panel report on nanostructure science and technology: R&D status and trends in nanoparticles, nanostructured materials, and nanodevices, International Technology Research Institute, p 49. (B) Zohari N, Keshavarz MH, Seyedsadjadi SA (2013) Central Eur J Energ Mat 10(1):135
68. (A) Patel R (2007) Insensitive munitions and energetic materials technology symposium, Miami, Florida. (B) Liu J, Jiang W, Li F, Wang L, Zeng J, Li Q, Wang Y, Yang Q (2014) Propellants Explos Pyrotech 39:30
69. (A) Stepanov V, Krasnoperov L, Elkina I, Zhang X (2005) Propellants Explos Pyrotech 30:178. (B) He B, Stepanov V, Qiu H, Krasnoperov LN (2015) Propellants Explos Pyrotech 40:659

70. Tappan BC, Brill TB (2003) Propellants, Explos, Pyrotech 28:223
71. Zhang Y, Liu D, Lv C (2005) Propellants, Explos, Pyrotech 30:438
72. Stepanov V, Anglade V, Hummers WAB, Bezmelnitsyn AV, Krasnoperov LN (2011) Propellants, Explos, Pyrotech 36:240
73. Redner P, Kapoor D, Patel R, Chung M, Martin D (2006) Production and characterization of nano-RDX. U.S. Army, RDECOM-ARDEC, Picatinny, NJ 07806-5000
74. Essel JT, Cortopassi AC, Kuo KK, Leh CG, Adair JH (2012) Propellants, Explos, Pyrotech 37:699
75. (A) Qiu H, Stepanov V, Chou T, Surapaneni A, Di Stasio AR, Lee WY (2012) Powder Technol 226:235. (B) Shi X, Wang J, Li X, An C, Central European Journal of Energetic Materials, 2014, 11(3), 433
76. An C, Li H, Guo W, Geng X, Wang J (2014) Propellants, Explos, Pyrotech 39:701
77. Zhang X, Weeks BL (2014) J Hazard Mater 268:224
78. Qiu H, Stepanov V, Di Stasio AR, Chou TM, Lee WY (2011) J Hazard Mater 185:489
79. (A) Armstrong RW, Coffey CS, DeVost VF, Elban WL (1990) J Appl Phys 68:979. (B) Wawiernia TM, Cortopassi AC, Essel JT, Ferrara PJ, Kuo KK (2009) 8th international symposium on special topics of chemical propulsion, Cape Town, South Africa, 2–6 Nov 2009
80. Shi X, Wang J, Li X, An C (2014) Central Eur J Energ Mat 11(3):433
81. Parrish DA, Deschamps JR, Gilardi RD, Butcher RJ (2008) Cryst Growth Des 8:57
82. Deschamps JR, Parrish DA (2015) Propellants, Explos, Pyrotech 40:506
83. Landenberger KB, Matzger AJ (2010) Cryst Growth Des 10:5341
84. Millar DIA, Maynard-Casely HE, Allan DR, Cumming AS, Lennie AR, Mackay AJ, Oswald IDH, Tang CC, Pulham CR (2012) Cryst Eng Comm 14(10):3742
85. Divekar CN, Sanghavi RR, Nair UR, Chakraborthy TK, Sikder AK, Singh A (2010) J Propul Power 26(1):120
86. Hikal WM, Bhattacharia SK, Weeks BL (2012) Propellants, Explos, Pyrotech 37:718
87. Lin H, Zhu S-G, Zhang L, Peng X-H, Li H-Z (2013) J Energ Mater 31(4):261
88. Bolton O, Matzger AJ (2011) Angew Chem 123:9122
89. Bolton O, Simke L, Pagoria P, Matzger A (2012) Cryst Growth Des 12:4311
90. Anderson SR, Ende DJ, Salan JS, Samuels P (2014) Propellants, Explos, Pyrotech 39:637
91. Li H, An C, Guo W, Geng X, Wang J, Xu W (2015) Propellants, Explos, Pyrotech 40:652
92. Jung JW, Kim KJ (2011) Ind Eng Chem Res 50(6):3475
93. Yang Z, Li J, Huang B, Liu S, Huang Z, Nie F (2014) Propellants, Explos, Pyrotech 39:51
94. Qiu H, Patel RB, Damavarapu RS, Stepanov V (2015) CrystEngComm 17:4080
95. McDonald BA (2011) Propellants, Explos, Pyrotech 36:576
96. Lin C-P, Chang Y-M, Gupta JP, Shu C-M (2010) Process Saf Environ Prot 88:413
97. Zayed MA, Hassan MA (2010) Propellants, Explos, Pyrotech 35:468
98. Zayed MA, El-Begawy SEM, Hassan HES (2013) Arab J Chem. doi:10.1016/j.arabjc.2013.08.021
99. Trache D, Khimeche K (2013) Fire Mater 37:328
100. Trache D, Khimeche K (2013) J Therm Anal Calorim 111:305
101. Jin B, Peng RF, Chu SJ, Huang YM, Wang R (2008) Propellants, Explos, Pyrotech 33:454
102. Pekker S, Kovats E, Oszlanyi G, Benyei G, Klupp G, Bortel G, Jalsovszky I, Jakab E, Borondics F, Kamaras K, Bokor M, Kriza G, Tompa K, Faigel G (2005) Nat Mater 4:764
103. Chi Y, Huang H, Li JS (2005) International autumn seminar on propellants, explosives and pyrotechnics (2005IASPEP), Beijing, China, 25–28 Oct 2005
104. Smeu M, Zahid F, Ji W, Guo H, Jaidann M, Abou-Rachid H (2011) J Phys Chem C 115:10985
105. Guo R, Hu Y, Shen R, Ye Y (2014) J Appl Phys 115:174901
106. (A) Hummers WS, Offeman RE (1958) J Am Chem Soc 80:1339. (B) Marcano DC, Kosynkin DV, Berlin JM, Sinitskii A, Sun ZZ, Slesarev A, Alemany LB, Lu W, Tour JM (2010) ACS NANO 4:4806

107. (A) Krishnan D, Kim F, Luo JY, Cruz-Silva R, Cote LJ, Jang HD, Huang JX (2012) Nano Today 7:137. (B) Kim F, Luo JY, Cruz-Silva R, Cote LJ, Sohn K, Huang JX (2010) Adv Funct Mater 20:2867
108. Li R, Wang J, Shen JP, Hua C, Yang GC (2013) Propellants, Explos, Pyrotech 38:798
109. Cowperthwaite M, Zwisler WH (1973) Tiger computer program documentation, Stanford Research Institute, Publication No. Z106
110. Freedman E (1988) Blake-A thermodynamics code based on TIGER: Users' Guide to the Revised Program, ARL-CR-422
111. Fried LE (1996) CHEETAH 1.39 User's manual, Lawrence Livermore National Laboratory, manuscript UCRL-MA-117541 Rev. 3
112. Sućeska M (1991) Propellants, Explos, Pyrotech 16:197–202
113. Grys S, Trzciński WA (2010) Central Eur J Energ Mat 7(2):97
114. Karir JS (2001) 28th International pyrotechnics seminar. 4–9 Nov 2001, Adelaide, South Australia
115. Xu F-M (2013) Defence Technol 9:127
116. Anderson RD, Rice BM (2000) Army research laboratory technical report ARL-TR-2326
117. (A) Klapötke TM, Stierstorfer J (2005) Proceedings of the 26th army science conference, Orlando, Florida, 1–4 Dec 2008. (B) Johnston IA (2005) Understanding and predicting gun barrel erosion, DSTO.TR.1757, Weapons Systems Division, Defence Science and Technology Organisation, Australia
118. Conroy PJ, Weinacht P, Nusca MJ (2001) Army research laboratory technical report, ARL-TR-2393
119. Conroy PJ, Leveritt CS, Hirvonen JK, Demaree JD (2006) Army research laboratory technical report, ARL-TR-3795
120. Doherty RM (2003) 9th IWCP on novel energetic materials and applications, Lerici (Pisa), Italy, 14–18 Sept 2003
121. Moxnes JF, Jensen TL, Smestad E, Unneberg E, Dullum O (2013) Propellants, Explos, Pyrotech 38:255
122. Rotariu T, Petre R, Zecheru T, Suceska M, Petrea N, Esanu S (2015) Propellants, Explos, Pyrotech 40:931
123. Jensen TL, Moxnes JF, Unneberg E, Dullum O (2014) Propellants, Explos, Pyrotech 39:830
124. Reese DA, Groven LJ, Son SF (2014) Propellants, Explos, Pyrotech 39:205
125. Liu B, Chen B, Yao Y-J, Wang Q-L, Yu H-F, Liu S-W (2015) Energy Procedia 66:121
126. Yao Y-J, Liu B, Wang Q-L, Liu S-W, Wei L, Zhang Y-B (2015) Energy Procedia 66:125
127. Martin R, Gonzalez A (1993) Proceedings of the JANNAF propulsion meeting. Monterey, California, 15–19 Nov 1993
128. Doali JO, Juhasz AA, Bowman RE, Aungst WP (1988) U.S. army ballistic research laboratory technical report, BRL-TR-2944
129. Cloutier T, Sadowski L (2005) Armament research, developments and engineering center, armaments engineering and technology center (Benet) technical report, ARAEW-TR-05006
130. Xiao Z-G, Ying S-J, Xu F-M (2014) Defence Technol 10:101
131. Li Y, Yang W, Ying S (2015) Propellants, Explos, Pyrotech 40:33
132. (A) Doali JO, Juhasz AA, Bowman RE, Aungst WP (1988) U.S. army ballistic research laboratory technical report, BRL-TR-2944. (B) Juhasz AA, May IW, Aungst WP, Doali JO, Bowman RE (1979) 16th JANNAF combustion meeting, Monterey, CA, USA, 10–14 Sept 1979. (C) May IW, Juhasz AA (1981) U.S. army ballistic research laboratory technical report, ARBRL-MR-03108. (D) Martin R, Gonzalez A (1993) JANNAF propulsion meeting, Monterey, CA, USA, 15–19 Nov 1993. (E) Cloutier T, Sadowski L (2005) Armament research, developments and engineering center, armaments engineering and technology center technical report, ARAEW-TR-05006. (F) Bonnet C, Pieta PD, Reynaud C (2001) 19th International symposium of ballistics, Interlaken, Switzerland, 7–11 May 2001

133. (A) Frolov YV, Korostelev V (1989) Propellants Explos Pyrotech 14:140. (B) Bçhnlein-Mauß J, Eberhardt A, Fischer TS (2002) Propellants Explos Pyrotech 27:156. (C) Bçhnlein-Mauß J, Krçber H (2009) Propellants Explos Pyrotech 34:239. (D) Kuo KK, Vichnevetsky R, Summerfield M (1973) AIAA J 11:444. (E) Kooker D, Anderson R (1981) 18th JANNAF combustion meeting, Pasadena, CA, USA, 19–23 Oct 1981. (F) James TB, Edward BF (1995) Army research laboratory technical report, ARL-CR-242
134. Yang W, Li Y, Ying S (2015) Propellants, Explos, Pyrotech 40:27
135. Yang W, Li Y, Ying S (2015) J Energ Mater 33:91–101
136. Su J, Ying S, Xiao Z, Xu F (2013) Propellants, Explos, Pyrotech 38(4):533
137. Jiang X-L, Liu T, Xu Z-M, Zhao L, Hu G-H, Yuan W-K (2009) J. Supercrit. Fluid 48:167
138. (A) Li Y, Yang W, Ying S (2014) Propellants Explos Pyrotech 39:677. (B) Li Y, Yang W, Ying S (2014) Propellants Explos Pyrotech 39:852
139. Li Y, Yang W, Ying S, Peng J (2015) J Energ Mater 33:167
140. Xiao Z, Ying S, Xu F (2010) Propellants, Explos, Pyrotech 35:1